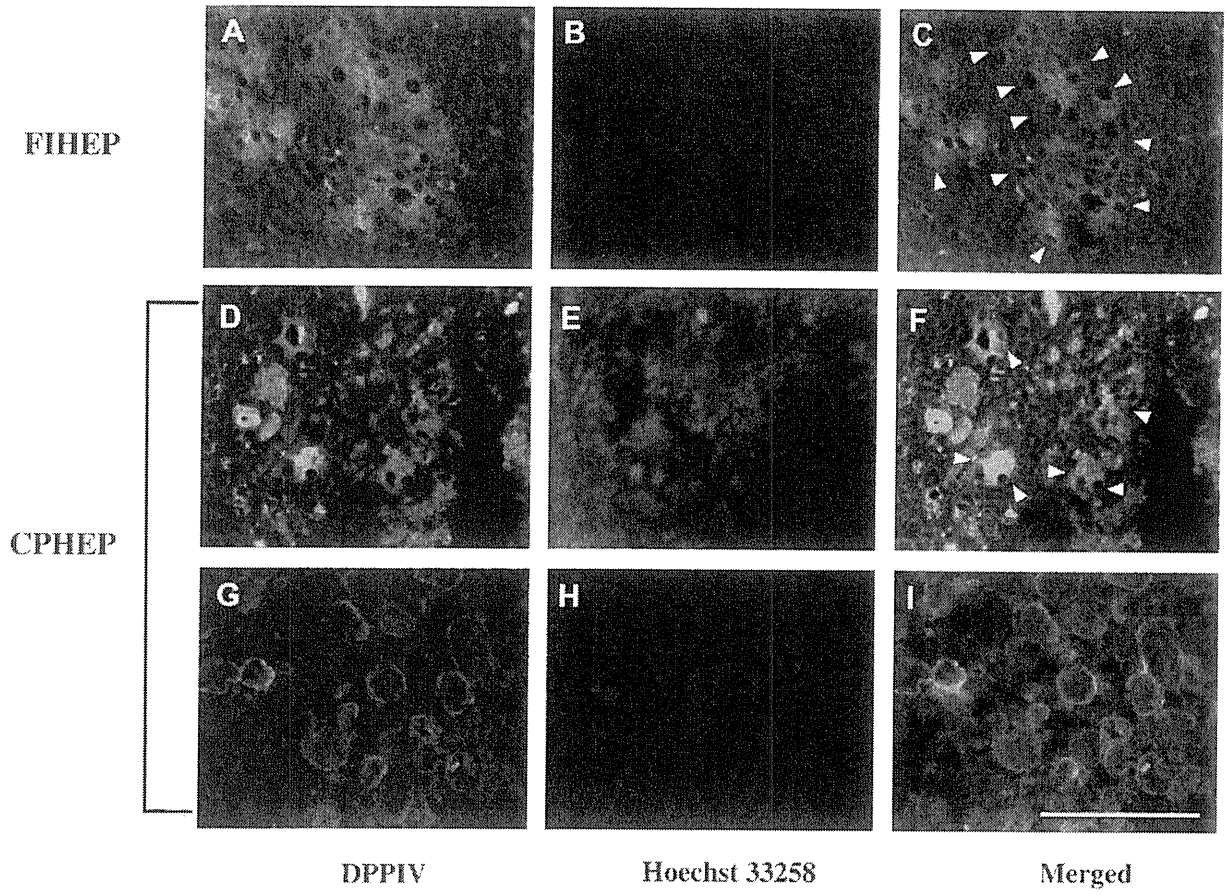

FIG. 3. Engraftment of the transplanted hepatocytes in the spleen of ALF rats. The rats were transplanted with FIHEPs (A)–(C) or CPHEPs (D)–(I) and subjected to ALF as in Figure 2B. Spleens were removed at 24 h after ALF induction and processed to cryosectioning for immunohistochemical analysis to detect DPPIV (green; A, D, G). The sections were counterstained with Hoechst 33258 [blue; (B), (E), (H)]. (A) and (B), (D) and (E), and (G) and (H) were merged into (C), (F), and (I), respectively. The arrowhead indicates $DPPIV^+$/$Hoechst\ 33258^+$ viable hepatocytes. Bar, 100 μm.

Blood Chemistry

Hepatocyte transplantation therapy for ALF was evaluated by measuring the blood levels of total bilirubin, GOT, GPT, NH_3, and Glu. The rats in the CM group showed higher levels of total bilirubin, GOT, GPT, and NH_3, and lower levels of Glu, than the hepatocyte-transplanted groups at 24 h post-ALF induction (Fig. 4), indicating that the rats experienced severe liver failure. FIHEP transplantation improved these biochemical data. The CPHEP groups showed improvement to an extent similar to the FIHEP groups. Total bilirubin and NH_3 values improved significantly, which strongly suggests that both engrafted FIHEPs and CPHEPs are functional in cholestasis and NH_3 metabolisms in ALF. However, neither FIHEP nor CPHEP transplantation significantly improved the levels of transaminase, suggesting that the transplanted hepatocytes were not sufficient to prevent ischemic changes induced by ligation of the liver lobes.

Concentrations of inflammatory cytokines in sera were also determined at 24 h post-ALF induction. TGF-β1 measured approximately 7 ng/mL, but IL-1β and IL-6 were not detected in sham-operated rats (Table 1). IL-1β and IL-6 levels in the CM group rose to approximately 300 pg/mL and 4000 pg/mL, respectively. TGF-β1 concentration in the CM group was approximately two times higher than that in sham-operated rats. IL-6 and TGF-β1 concentrations in the FIHEP and CPHEP groups became significantly lower than those in the CM group, although IL-1β concentration did not (Table 1).

Proliferation of the Remnant Liver Hepatocytes Post-ALF Induction

Hepatocyte transplantation increased the host's lifespan, suggesting that the hepatocytes in the remnant liver might be stimulated to proliferate or their cell death rates might decrease despite no gain in liver

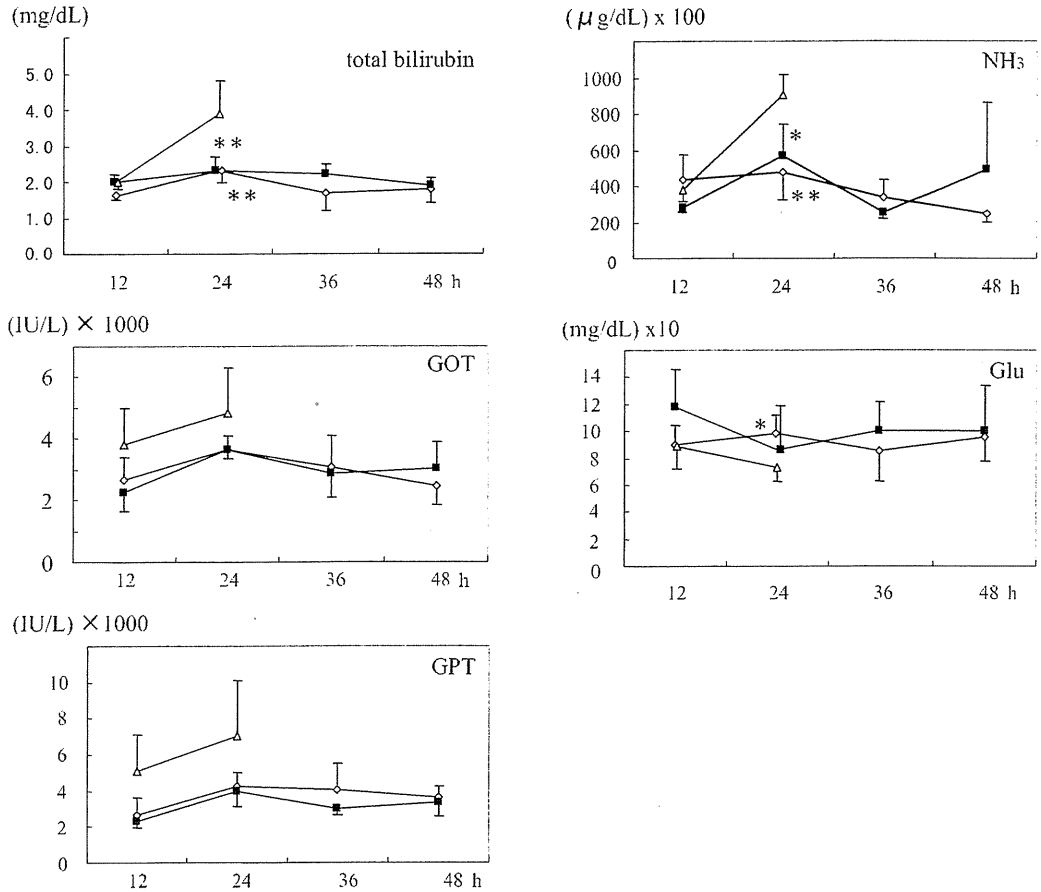

FIG. 4. Biochemical evaluation of hepatocyte transplantation therapy for ALF. The rats were subjected to hepatocyte transplantation and ALF treatment as described in Figure 2. At the indicated time points after ALF treatment, blood was collected for total bilirubin, NH_3, GOT, Glu, and GPT assessment. The mean values of total bilirubin, GOT, GPT, NH_3, and Glu in the normal control rats were 0.3 ± 0.1 (mg/dL), 75 ± 18 (IU/L), 25 ± 6 (IU/L), 151 ± 23 (μg/dL), and 197 ± 26 (mg/dL), respectively. The open diamond, closed rectangle, and open triangle indicate the FIHEP, CPHEP, and CM groups, respectively. $^*P < 0.05$ *versus* the CM group. $^{**}P < 0.01$ *versus* the CM group.

weight within the experimental period (up to 5 d). To address this possibility, the BrdU-labeling index and TUNEL activity were determined as a measure of cell proliferation activity and cell death, respectively. BrdU-labeling indexes at 24 h post-ALF in the CM, FIHEP, and CPHEP groups are shown in Figure 5A-1, A-2, and A-3, respectively. $BrdU^+$ nuclei were present in the FIHEP and CPHEP groups but were scarce in the CM group. These $BrdU^+$ hepatocytes were host hepatocytes because they were $DPPIV^-$. The BrdU-labeling indexes are shown in Figure 5A-4. The indexes at 12 h were low (<2%) and not significantly different among the three groups of rats. The indexes of the FIHEP and CPHEP groups at 24 h significantly increased, compared with those of the CM group. At 48 h post-ALF, there was a similarly large increase in the labeling indexes (>10%) in both the FIHEP and CPHEP rat livers, indicating that CPHEP transplantation stimulated the proliferation of the remnant hepatocytes as effectively as FIHEP transplantation. In a parallel experiment, some sections at 24 h post-ALF were stained for TUNEL activity. $TUNEL^+$ hepatocytes were frequently observed in the CM rats (Fig. 5B-1) but decreased substantially in the FIHEP (Fig. 5B-2) and CPHEP (Fig. 5B-3) rats. The ratios of the $TUNEL^+$ hepatocytes to the total hepatocytes are shown in Figure 5B-4 as apoptotic indexes. The apoptotic index

TABLE 1

Comparison of Inflammatory Cytokines 24 h Post-ALF Induction

Exp. group	IL-1β (pg/mL)	IL-6 (pg/mL)	TGF-β1 (ng/mL)
SO	ND	ND	7.27 ± 3.16
FIHEP	382.1 ±107.3	499.8 ± 485.6	10.56 ± 4.21*
CPHEP	418.1 ± 73.8	337.4 ± 150.7*	10.79 ± 1.94*
CM	329.1 ± 32.8	4375.5 ± 5568.9	15.27 ± 2.74

ALF = acute liver failure; SO = sham operation; ND = not detected. FIHEP = freshly isolated hepatocyte; CPHEP = culture-propagated hepatocyte; CM = culture medium

Sham operation indicates laparotomy alone.

$^*P < 0.05$ *versus* the CM group.

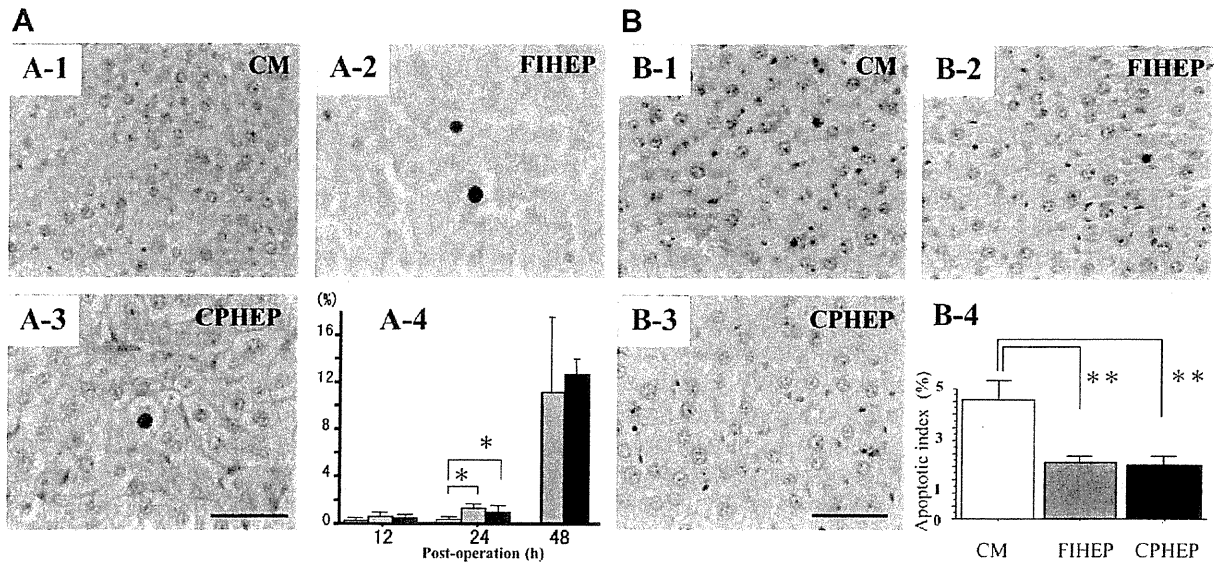

FIG. 5. (A) BrdU-labeling index of hepatocytes in the remnant liver of the hepatocyte- transplanted rat. The rats were injected with CM, transplanted with FIHEPs or CPHEPs, and subjected to ALF as in Fig. 2. The remnant livers (omental lobe) were removed at 12, 24, and 48 h post-induction of ALF and processed to obtain paraffin sections for BrdU staining. (A-1), (A-2), and (A-3) are representative of photos from rats with CM, FIHEPs, and CPHEPs, respectively, taken at 24 h post-ALF. $BrdU^+$ nuclei are brown in color. In (A-4), $BrdU^+$ cells were counted from five microscopic fields of each section from 4 rats in each group at the time points indicated, and the BrdU-labeling index was calculated as the ratio of $BrdU^+$ cells to the total cells in a counted field. The open bar, gray bar, and black bar indicate the CM, FIHEP, and CPHEP groups, respectively. $*P < 0.05$ *versus* the CM group. Bar, 50 μm. (B) Suppression of remnant hepatocyte apoptosis by hepatocyte transplantation. The rats were transplanted with hepatocytes and subjected to ALF as described in Fig. 2. Paraffin sections were prepared from the remnant livers (omental lobes) isolated from the CM (B-1), FIHEP (B-2), and CPHEP groups (B-3) at 24 h post-ALF and were stained for TUNEL activity. $TUNEL^+$ pycnotic nuclei (brown) were frequently observed in the CM group, but less often in the FIHEP and CPHEP groups. Apoptotic cells were counted from five microscopic fields of liver tissue sections from four rats in each group. The ratio of apoptotic cells to total cells in the counted field was expressed as the apoptotic index (B-4). The open bar, gray bar, and black bar indicate the CM, FIHEP, and CPHEP groups, respectively. $**P < 0.01$ *versus* the CM group. Bar, 50 μm.

of the remnant liver in the FIHEP and CPHEP groups decreased to approximately 50% of that in the CM group. These $TUNEL^+$ hepatocytes were host hepatocytes because they were $DPPIV^-$. Thus, CPHEP transplantation suppressed the apoptotic changes in the host hepatocytes as effectively as FIHEP transplantation.

DISCUSSION

Although several studies have supported the effectiveness of hepatocyte transplantation in treating patients with ALF, there is a severe problem in using hepatocyte transplantation therapy as a general clinical treatment for patients with liver failure: owing to the lack of donor organs available for clinical use, hospitals cannot supply sufficient quantities of normal human hepatocytes to such patients. One way to overcome this limitation might be to devise a method of abundantly propagating hepatocytes in culture, starting with a small amount of hepatocytes isolated from small pieces of available liver tissues. However, it does not seem to be a practical solution, because it is well documented that normal hepatocytes show poor multiplication ability *in vitro* despite their remarkable growth potential *in vivo* [19].

We have been engaged in developing a technology to abundantly propagate hepatocytes in culture [8, 9] and previously reported that rat hepatocytes were capable of repeatedly multiplying *in vitro* when cocultured with Swiss 3T3 cells in a medium that we devised [10]. We have now shown that such CPHEPs can be used as a source of hepatocyte transplantation for preventing hepatectomy-induced ALF. Resection of hepatic tumors is currently the gold standard treatment for patients with either primary or secondary liver malignancies. An extended hepatectomy is often necessary to achieve curative resection; however, ALF after massive hepatectomy remains a challenging problem (i.e., the risk of insufficiency of remnant liver volume, leading to unresectability). If we devise a countermeasure to prevent ALF beforehand, aggressive hepatic resection could be safely performed. Seeking to answer this clinical question, we evaluated the prevention efficacy of CPHEP transplantation in a surgical model of hepatectomy-induced ALF.

To estimate the efficacy of transplanting either FIHEPs or CPHEPs in ALF, we employed an experimental ALF model induced by subjecting rats to two-thirds-hepatectomy and ligation of the right-lobe pedicle. This method induces more severe liver failure than

a model induced by 90% hepatectomy and is considered to mimic the clinical status of human ALF fairly faithfully [14]. The rats lacked a functional liver and showed ischemic changes in the right lobe, resulting in regeneration failure of the remnant omental lobe, whose weight occupied about 8% of the total liver weight. This model has previously been used to demonstrate that FIHEP transplantation effectively prolongs the survival of rats suffering from ALF [15]. We reproduced similar results in the present study. Notably, CPHEPs, which had been prepared by multiplying FIHEPs 3 times, were as effective as FIHEPs in prolonging the survival of rats suffering from ALF. CPHEP transplantation improved all the liver functions tested in this study. In addition, the BrdU-labeling index of the hepatocytes in the remnant liver was comparable to that in the FIHEP group. Rats with CPHEPs gradually regained liver weight after ALF induction, as did those with FIHEPs. These results together indicate that both CPHEP and FIHEP could be a source for hepatocyte transplantation to promote regeneration of the remnant liver after ALF induction.

There have been two explanations for lethal hepatic failure after excessive hepatectomy: hepatectomy causes microcircular disturbances [20] or induces cytotoxic factors such as TNF-α, TGF-β1, and oxidative stress-related factors [21, 22]. In the present study, we did not find any evidence of microvascular disturbances on hematoxylin and eosin (H&E)-stained sections of the remnant lobe in the ALF-induced rats, but we did observe hypercytokinemia of cytokines such as IL-6 and TGF-β1. Apoptotic hepatocytes were frequently seen by TUNEL assay in the remnant liver lobe of the ALF-induced rats. CPHEP and FIHEP transplantation decreased the concentrations of IL-6 and TGF-β1 in sera, as well as the frequency of apoptotic hepatocytes. Therefore, it appears that both CPHEPs and FIHEPs prolonged the survival of ALF-induced rats by suppressing the hepatocytic apoptosis in the remnant liver.

In the present study, we demonstrated the presence of DPPIV$^+$ hepatocytes in the spleen at 24 h after ALF induction, which clearly indicated the engraftment of both transplanted CPHEPs and FIHEPs in the graft site. There were no significant differences in the frequency of DPPIV$^+$ hepatocytes between the FIHEP and CPHEP groups. However, the expression level of hepatocyte-specific mRNAs such as Alb, CYP2C7, and GS in the spleen of the CPHEP rats was considerably lower than that in the FIHEP rats. This might be explained by the fact that CPHEPs showed lower expression levels of these marker genes than FIHEPs at the time of transplantation; this was due to the fact that the CPHEP cells had been cultured for 11 d before transplantation, during which time the expression levels had decreased (Fig. 1B). Another explanation could be that the CPHEPs were more vulnerable than the FIHEPs, and that most of them became nonviable in the spleen after transplantation. We noticed the presence of many DPPIV$^+$ but Hoechst$^-$ cells in the middle of the CPHEP clusters, but not in the FIHEP clusters. These Hoechst$^-$ cells were considered to be nonviable.

It has previously been shown that homogenized hepatocytes were even effective as a treatment for liver failure [23], suggesting the effectiveness of nonviable hepatocytes. In the present study, we also showed that the survival rate of the rats in the DHEP group was better, to some extent, than that in the control CM group, although the rate was much lower than that of the CPHEP group. In light of these results, it is likely that transplanted CPHEPs contribute to the improvement of liver failure by substituting the function of the host liver. They may also provide some growth factors or enzymes to support the regeneration of the remnant liver. It remained to be elucidated whether the cryopreserved CPHEPs also display such beneficial effects. Hepatocytes are known to be very sensitive to freezing damage. Three distinct modes of cryopreservation-induced hepatocyte death have been identified, namely, physical cell rupture, necrosis, and apoptosis [24]. The susceptibility of hepatocytes to such freeze-thaw injury is attributed to the damage to mitochondria, including loss of mitochondrial membrane integrity, increase in membrane permeability, etc. The inhibition of mitochondria damage, for instance, by broad-spectrum caspase-inhibitor, would prevent cryopreservation-induced damage of propagated hepatocytes.

In conclusion, the transplantation of homologous CPHEPs has a remarkable therapeutic potential for ALF in rats. Since we have recently established a culture method that enables us to multiply human hepatocytes 50 to 100 times during 50 d of culture [25], CPHEPs might be a useful source of hepatocytes for transplantation to treat human patients with ALF.

REFERENCES

1. Lee WM. Acute liver failure. N Engl J Med 1993;329:1862.
2. Bismuth H, Samuel D, Casting D, et al. Orthotopic liver transplantation in fulminant and subfulminant hepatitis. Ann Surg 1995;222:109.
3. Moreno GE, Garcia GI, Loinaz SC, et al. Liver transplantation in patients with fulminant hepatic failure. Br J Surg 1995;82:118.
4. Gewartowska M, Olszewski WL. Hepatocyte transplantation-biology and application. Ann Transplant 2007;12:27.
5. Habibullah MC, Syde HI, Qamar A, et al. Human fetal hepatocyte transplantation in patients with fulminant hepatic failure. Transplantation 1994;58:951.
6. Strom SC, Fisher RA, Thompson MT, et al. Hepatocyte transplantation as a bridge to orthotopic liver transplantation in terminal liver failure. Transplantation 1997;63:559.

7. Fisher RA, Bu D, Thompson M, et al. Defining hepatocellular chimerism in liver failure patient bridge with hepatocyte infusion. Transplantation 2000;69:303.
8. Tateno C, Yoshizato K. Long-term cultivation of adult rat hepatocytes that undergo multiple cell divisions and express normal parenchymal phenotypes. Am J Pathol 1996;148:383.
9. Tateno C, Takai-Kajihara K, Yamasaki C, et al. Heterogeneity of growth potential of adult rat hepatocytes *in vitro*. Hepatology 2000;31:65.
10. Sato H, Funahashi M, Kristensen DB, et al. Pleiotrophin as a Swiss 3T3 cell-derived potent mitogen for adult rat hepatocytes. Exp Cell Res 1999;246:152.
11. Hino H, Tateno C, Sato H, et al. A long-term culture of human hepatocytes which show a high growth potential and express their differentiated phenotypes. Biochem Biophys Res Commun 1999;256:184.
12. Seglen PO. Preparation of isolated rat liver cells. Methods Cell Biol 1976;13:29.
13. Katayama S, Tateno C, Asahara T, et al. Size-dependent *in vivo* growth potential of adult rat hepatocytes. Am J Pathol 2001; 158:97.
14. Eguchi S, Lilja H, Hewitt W, et al. Loss and recovery of liver regeneration in rats with fulminant hepatic failure. J Surg Res 1997;72:112.
15. Eguchi S, Kamolt A, Ljubiova J, et al. Fulminant hepatic failure in rats: Survival and effects on blood chemistry and liver regeneration. Hepatology 1996;24:1452.
16. Higgins GM, Anderson RM. Experimental pathology of the liver. 1. Restoration of the liver of the white rat following partial surgical removal. Arch Pathol 1931;12:186.
17. Gordon GJ, Coleman WB, Hixon DC, et al. Liver regeneration in rats with retrosine-induced hepatocellular injury proceeds through a novel cellular response. Am J Pathol 2000; 156:607.
18. Asahina K, Sato H, Yamasaki C, et al. Pleiotrophin/heparin-binding growth-associated molecule as a mitogen of rat hepatocytes and its role in regeneration and development of liver. Am J Pathol 2002;160:2191.
19. Fausto N, Campbell JS, Riehle KJ. Liver regeneration. Hepatology 2006;43(2 Suppl. 1):45.
20. Kamimukai N, Togo S, Hasegawa S, et al. Expression of Bcl-2 family reduces apoptotic hepatocytes after excessive hepatectomy. Eur Surg Res 2001;33:8.
21. Leist M, Gantner F, Bohlinger I, et al. Tumor necrosis factor-induced hepatocyte apoptosis precedes liver failure in experimental murine shock models. Am J Pathol 1995;146:1220.
22. Oberhammer FA, Pavelka M, Sharma S, et al. Induction of apoptosis in culture hepatocytes and in regressing liver by transforming growth factor β1. Proc Natl Acad Sci U S A 1992; 89:5408.
23. Grundmann R, Koebe HG, Waters W. Transplantation of cryopreserved hepatocytes or liver cytosol injection in the treatment of acute liver failure in rats. Res Exp Med 1986; 186:141.
24. Terry C, Dhawan A, Mitry RR, Hughes RD. Cryopreservation of isolated human hepatocytes for transplantation: State of the art. Cryobiology 2006;53:149.
25. Yamasaki C, Tateno C, Aratani A, et al. Growth and differentiation of colony-forming human hepatocytes in vitro. J Hepatol 2006;44:749.

Growth Hormone-Dependent Pathogenesis of Human Hepatic Steatosis in a Novel Mouse Model Bearing a Human Hepatocyte-Repopulated Liver

Chise Tateno, Miho Kataoka, Rie Utoh, Asato Tachibana, Toshiyuki Itamoto, Toshimasa Asahara, Fuyuki Miya, Tatsuhiko Tsunoda, and Katsutoshi Yoshizato

Yoshizato Project (C.T., M.K., R.U., A.T., K.Y.), Hiroshima Prefectural Institute of Industrial Science and Technology, Cooperative Link of Unique Science and Technology for Economy Revitalization (CLUSTER), and PhoenixBio, Co. Ltd. (C.T., A.T., K.Y.), Higashihirosima, Hiroshima 739-0046, Japan; Hiroshima University Liver Project Research Center (C.T., T.A., K.Y.) and Division of Frontier Medical Science (T.I., T.A.), Department of Surgery, and Hiroshima University 21st Century COE Program for Advanced Radiation Casualty Medicine, Programs for Biomedical Research, Graduate School of Biomedical Sciences, Hiroshima University, Hiroshima, Hiroshima 734-8551, Japan; Laboratory for Medical Informatics (F.M., T.T.), Center for Genomic Medicine, RIKEN, Yokohama, Kanagawa 230-0045, Japan; Developmental Biology Laboratory and Hiroshima University 21st Century COE Program for Advanced Radiation Casualty Medicine (K.Y.), Department of Biological Science, Graduate School of Science, Hiroshima University, Higashihiroshima, Hiroshima 739-8526, Japan; and Departments of Hepatology and Liver Research Center (K.Y.), Graduate School of Medicine, Osaka City University, Osaka 545-8586, Japan

Clinical studies have shown a close association between nonalcoholic fatty liver disease and adult-onset GH deficiency, but the relevant molecular mechanisms are still unclear. No mouse model has been suitable to study the etiological relationship of human nonalcoholic fatty liver disease and human adult-onset GH deficiency under conditions similar to the human liver *in vivo*. We generated human (h-)hepatocyte chimeric mice with livers that were predominantly repopulated with h-hepatocytes in a h-GH-deficient state. The chimeric mouse liver was mostly repopulated with h-hepatocytes about 50 d after transplantation and spontaneously became fatty in the h-hepatocyte regions after about 70 d. Infusion of the chimeric mouse with h-GH drastically decreased steatosis, showing the direct cause of h-GH deficiency in the generation of hepatic steatosis. Using microarray profiles aided by real-time quantitative RT-PCR, comparison between h-hepatocytes from h-GH-untreated and -treated mice identified 14 GH-up-regulated and four GH-down-regulated genes, including *IGF-I*, *SOCS2*, *NNMT*, *IGFLS*, *P4AH1*, *SLC16A1*, *SRD5A1*, *FADS1*, and *AKR1B10*, respectively. These GH-up- and -down-regulated genes were expressed in the chimeric mouse liver at lower and higher levels than in human livers, respectively. Treatment of the chimeric mice with h-GH ameliorated their altered expression. h-Hepatocytes were separated from chimeric mouse livers for testing *in vitro* effects of h-GH or h-IGF-I on gene expression, and results showed that GH directly regulated the expression of *IGF-I*, *SOCS2*, *NNMT*, *IGFALS*, *P4AH1*, *FADS1*, and *AKR1B10*. In conclusion, the chimeric mouse is a novel h-GH-deficient animal model for studying *in vivo* h-GH-dependent human liver dysfunctions. **(*Endocrinology* 152: 1479–1491, 2011)**

To study pathophysiological characteristics of the human liver, we previously generated a humanized (chimeric) mouse whose liver was almost completely repopulated with human (h-)hepatocytes by transplanting h-hepatocytes into immunodeficient and liver-damaged mice, which had been obtained by mating an albumin enhancer/promoter-driven

ISSN Print 0013-7227 ISSN Online 1945-7170
Printed in U.S.A.

doi: 10.1210/en.2010-0953 Received August 18, 2010. Accepted January 10, 2011.
First Published Online February 8, 2011

Abbreviations: AGHD, Adult-onset GH deficiency; Alb, albumin; CK, cytokeratin; GO, gene ontology; h-, human; m-, mouse; 9MM, 9-month-old male; NAFLD, nonalcoholic fatty liver disease; NASH, nonalcoholic steatohepatitis; ORO, Oil Red O; qRT-PCR, quantitative RT-PCR; RI, replacement index; SCID, severe combined immunodeficient; uPA, urokinase-type plasminogen-activator; 25YF, 25-yr-old female; 61YF, 61-yr-old female; 28YM, 28-yr-old male; 57YM, 57-yr-old male.

urokinase-type plasminogen-activator (uPA) transgenic mouse with a severe combined immunodeficient (SCID) mouse (uPA/SCID mouse) (1–3). The replacement index (RI), the occupancy ratio of h-hepatocytes to the total [h- and mouse (m-)] hepatocytes in the chimeric mouse liver, indicated the degree of replacement with h-hepatocytes. The RI in the mice was as high as 96% (1). h-Hepatocytes therein expressed mRNA for drug-metabolizing enzymes and transporters as in donor livers (1, 4, 5). However, we noticed that the mice spontaneously developed hepatic steatosis as the time after transplantation was prolonged. The h-hepatocytes of a chimeric mouse are in a GH-deficient state (6) primarily because human cells do not react with rodent GH (7), thus suggesting that the observed lipid accumulation in h-hepatocytes was caused by a lack of available h-GH in chimeric mice.

A concern is increasing about nonalcoholic fatty liver disease (NAFLD) as a significant complication of obesity and as a hepatic manifestation of the metabolic syndrome (8). There are striking similarities between obesity and untreated adult-onset GH deficiency (AGHD), indicating that homeostatic imbalance of GH is an etiological factor of obesity (9). NAFLD is related to hypopituitary and hypothalamic dysfunction (10–12). AGHD is featured as decrease in body mass, increase in visceral adiposity, and abnormal lipid profile (13), which are associated with hepatic steatosis (11, 13, 14). One study showed that reduction in GH concentration was a predictor of NAFLD in adult males (15) and another that GH administration drastically improved the fatty liver of AGHD patients (13, 14). A suitable GH-dependent lipogenetic animal model is currently absent, in which we can investigate the *in vivo* effects of h-GH on h-hepatocytes at the cellular and molecular levels.

In this study, we first tested the hypothesis that h-hepatocytes in chimeric mouse liver develop steatosis due to the lack of circulating h-GH. In fact, hepatic steatosis was induced in the mouse liver but not when the chimeric mice were treated with h-GH. We then compared gene expression profiles between h-GH-treated and -untreated chimeric mouse h-hepatocytes to identify h-GH-regulated lipogenesis genes. Furthermore, we examined whether h-GH directly regulates the expression of lipogenesis-related genes or of h-IGF-I levels using cultured chimeric mouse h-hepatocytes. As a whole, the chimeric mouse was proved to be a suitable animal model for studying the etiological relationship among AGHD, GH, and NAFLD in GH-related aspects of metabolic syndrome.

Materials and Methods

We performed studies under the ethical approval of the Hiroshima Prefectural Institute of Industrial Science and Technology Ethics Board and the Ethics Committee at the Hiroshima University Hospital.

Preparation of h-hepatocytes

Livers were obtained from four donors [a 28-yr-old male (28YM) and a 57-yr-old male (57YM) and a 25-yr-old female (25YF) and a 61- yr-old female (61YF)] after receiving informed consent before surgery, according to the 1975 Declaration of Helsinki. h-Hepatocytes were isolated from the liver tissues as previously reported (1). Real-time quantitative RT-PCR (qRT-PCR) was performed on these human livers and/or on h-hepatocytes isolated from h-liver tissues (Table 1).

Donor cells for chimeric mice were h-hepatocytes from a Caucasian 9-month-old male (9MM) infant and an African-American 6-yr-old girl (6YF) purchased from In Vitro Technologies (Baltimore, MD) and BD Biosciences Discovery Labware (San Jose, CA), respectively.

Animals, transplantation of h-hepatocytes, and treatment of chimeric mice with h-GH

Production of uPA/SCID mice (1) and examination of their zygosity in uPA transgenes (16) were performed as previously reported. Homozygotic mice (20–30 d old) were used as hosts for all transplantation experiments. The 9MM and 6YF hepatocytes (hepatocytes$_{9MM}$ and hepatocytes$_{6YF}$, respectively), 7.5–10.0 $\times$ 10^5 cells per animal, were transplanted into six uPA/SCID mice (Table 2) for microarray and real-time qRT-PCR analysis and into 41 mice [36 mice for steatosis analysis (Fig. 1C) and five mice for steatosis analysis under h-GH treatment (Fig. 2E)], as previously described (1). Chimeric mice were killed 48–118 d after transplantation.

Three chimeric mice with hepatocytes$_{9MM}$ [nos. 4–6 (Table 2)], three chimeric mice with hepatocytes$_{6YF}$ [nos. 4–6 (Table 2)], one chimeric mouse$_{9MM}$ (not included in Table 2), and one chimeric mouse$_{6YF}$ (not included in Table 2) were continuously infused with 2.5 mg/kg·d h-GH (Wako, Osaka, Japan) through an sc-implanted Alzet micro-osmotic pump (Alza Corp., Palo Alto, CA) for 2 wk before killing (6, 17). Blood h-albumin (Alb) and serum h-IGF-I in the mice were quantified as previously reported (6).

Immunohistochemistry, lipid staining, and grading of steatosis in h-hepatocytes of chimeric mouse liver

Formalin-fixed paraffin sections from the left lateral lobe of six chimeric mice$_{6YF}$ were stained with mouse anti-h-cytokeratin (CK) 18 monoclonal antibodies (clone CD10; Dako Cytomation, Glostrup, Denmark) that did not react m-hepatocytes as

TABLE 1. Human liver tissues used in real-time qRT-PCR

Objectives	Age (yr)	Sex	RT-PCR
25YF	25	F	Cell and tissue
28YM	28	M	Cell and tissue
57YM	57	M	Cell
61YF	61	F	Cell and tissue

F, Female; M, male.

TABLE 2. Chimeric mice used in microarray analysis and real-time qRT-PCR

Donors	Animal number (sex)	Treatment with h-GH[a]	Days after transplantation	h-Alb in blood (mg/ml)	h-IGF-I in sera (ng/ml)	RI_{Alb} (%)[b] or RI_{immuno} (%)[c]	Microarray or RT-PCR
9MM	1 (F)	−	72	16.1	ND	>95[b]	Cell
	2 (F)	−	75	10.4	ND	>95[b]	
	3 (F)	−	101	6.0	ND	80[b]	
	4 (M)	+	75	8.1	ND	95[b]	
	5 (F)	+	75	6.2	ND	80[b]	
	6 (F)	+	75	5.9	ND	80[b]	
6YF	1 (F)	−	97	3.5	<9.4	75.1[c]	Tissue
	2 (F)	−	90	6.5	<9.4	78.1[c]	
	3 (F)	−	111	5.2	<9.4	70.2[c]	
	4 (M)	+	84	5.3	69.6	85.3[c]	
	5 (F)	+	84	3.7	64.8	70.3[c]	
	6 (F)	+	84	5.9	83.0	81.5[c]	

F, Female; M, male; ND, not determined.

[a] −, untreated with h-GH; +, treated with hGH.

[b] RI calculated by the blood h-Alb levels using the formula of the correlation curve $y = 0.0006x^2 + 0.0281x - 0.0042$ ($r^2 = 0.60$) in which x and y represent RI and blood h-Alb level, respectively.

[c] RI determined by immunohistological staining of liver sections.

previously described (18). The area occupied by h-CK18-positive (h-CK18$^+$) hepatocytes was identified to calculate RI (1).

Frozen sections were prepared from the livers of five h-GH-treated and 36 chimeric h-GH-untreated $mice_{6YF}$ and stained with Oil Red O (ORO). When necessary, serial sections were stained with anti-h-CK8/18 antibodies (MP Biomedicals, Aurora, OH) that did not react with m-hepatocytes as previously described (19). Steatosis grading of h-hepatocytes was performed on ORO-stained chimeric mouse liver sections as follows: grade 0, no lipid droplets; grade 1, appearance of small lipid droplets; grade 2, small and middle-sized lipid droplets; grade 3, small to large droplets (Fig. 1B).

Isolation of h-hepatocytes from chimeric mouse livers for gene expression profiles

Livers were isolated 72–101 d after transplantation from h-GH-untreated control chimeric $mice_{9MM}$ [nos. 1–3 (Table 2)] and h-GH-treated chimeric $mice_{9MM}$ [nos. 4–6 (Table 2)]. These livers were disaggregated by two-step collagenase perfusion as previously described (20), except perfusion was for 20 min and centrifugation was three times 2 min at 50 × *g*. Pelleted hepatocytes (h-$hepatocytes_{chimeric\ mouse}$) were treated with RLT buffer solution in an RNeasy Mini kit (QIAGEN K.K., Tokyo, Japan) and stored in a deep freezer until RNA isolation for microarray and real-time qRT-PCR.

Purity of h-hepatocytes$_{chimeric\ mouse}$

We previously established the correlation curve for chimeric $mice_{9MM}$ between the blood h-Alb concentration and RI_{immuno}, which is determined immunohistologically from liver tissue sections (1). The correlation curve predicted that chimeric $mice_{9MM}$ for microarray and real-time qRT-PCR examinations had a RI_{Alb} higher than 80% (Table 2). Apparently, this RI was a lower estimation of the real h-hepatocyte purity in hepatocyte preparations because m-hepatocytes were often lost during collagenase digestion due to fragility against the enzyme. Thus, the correct h-hepatocyte purity in the $hepatocytes_{chimeric\ mouse/9MM}$ (hepatocytes isolated from chimeric mouse liver bearing h-$hepatocytes_{9MM}$) was determined as follows. Among chimeric $mice_{6YF}$, we selected 10 mice whose RI_{Alb} at the time of death was similar to that of the chimeric $mice_{9MM}$ and isolated h-$hepatocytes_{chimeric\ mouse}$ from them. They were incubated with K8216 antibodies that react with the cell surface of h- but not m-hepatocytes (21) and then with secondary antibody, followed by fluorescence-activated cell sorting analysis to determine the percentage of h-hepatocytes in the $hepatocytes_{chimeric\ mouse}$. The h-hepatocyte purity was 90.8 ± 6.4% (n = 10). The presence of m-hepatocytes in $hepatocytes_{chimeric\ mouse}$ at less than 10% did not affect microarray assays as described in *Results*.

Microarray analysis

RNAs were extracted using TRIzol reagent (Invitrogen, Carlsbad, CA) from h-hepatocytes and h-liver tissues isolated from h-GH-untreated and -treated chimeric mice and were used for microarray analysis at the hepatocyte and liver tissue levels, respectively (Table 2). The array profiles were compared between h-GH-treated and -untreated samples, and statistical significance tests were performed. We deposited our array data to NCBI GEO (Gene Expression Omnibus, http://www.ncbi.nlm.nih.gov/geo/query/acc.cgi?acc=GSE26224, GEO ID GSE26224).

Microarray at the hepatocyte level

Six chimeric $mice_{9MM}$ [nos. 1–6 (Table 2)] were used in the hepatocyte level microarray assay. Half of the chimeric mice (nos. 1–3) were as h-GH-untreated control animals and the remaining half (nos. 4–6) as h-GH-treated animals by treating with h-GH during the last 2 wk before killing. h-$Hepatocytes_{chimeric\ mouse}$ were isolated from h-GH-untreated and -treated chimeric $mice_{9MM}$ at 72–101 d and 75 d after transplantation, respectively, for total RNA isolation.

The RNA samples were treated with deoxyribonuclease (QIAGEN K.K.), purified using ribonuclease-free deoxyribonuclease set (QIAGEN K.K.) and RNeasy Mini Kit (QIAGEN K.K.), and applied to an Affymetrix GeneChip Human Genome U133 Plus 2.0 Array (Affymetrix, Santa Clara, CA) that had been spotted with 54,675 human transcripts. Microarray data were normalized using GCOS software version 1.3 (Affymetrix). The

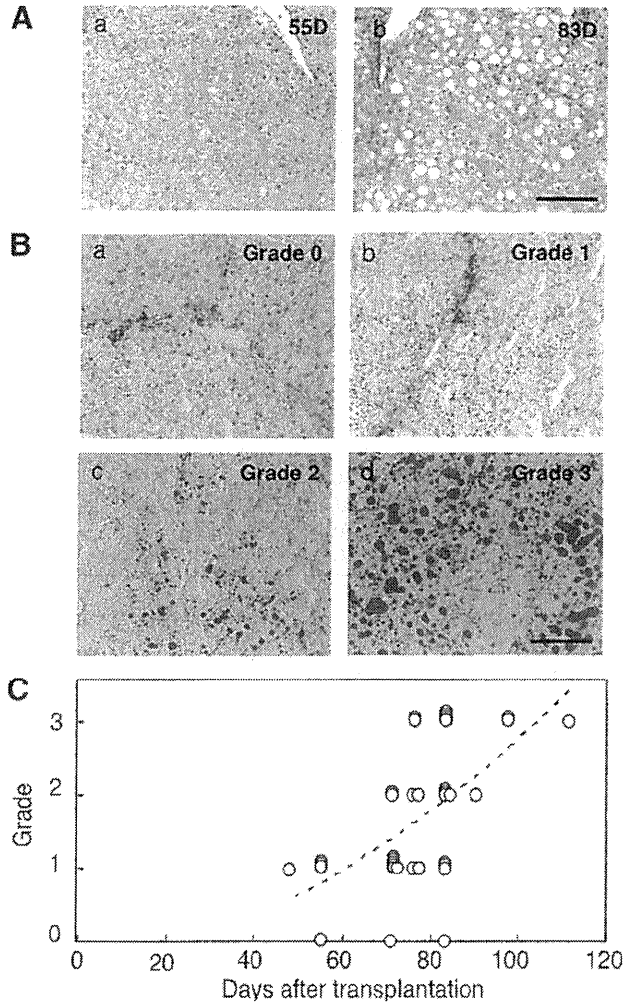

FIG. 1. Lipid accumulation in chimeric mouse h-hepatocytes. Chimeric mice$_{6YF}$ were killed 48–111 d after transplantation for histological examinations by hematoxylin and eosin (A) and ORO liver staining (B). A, h-Hepatocyte regions in the mice killed at 55 d (55D) (a) and 83 d (83D) (b). No visible cytoplasmic vacuolation in the h-hepatocytes at 55 d, but extensive and intensive vacuolation at 83 d. B, Grading of steatosis. Photos of typical staining show various levels of lipid accumulation with nuclei stained *blue*. Lipid accumulation was graded as described in the text: a, grade 0 (55 d); b, grade 1 (77 d); c, grade 2 (83 d); d, grade 3 (97 d). *Bars*, 100 μm. C, Relationship between steatosis grade and duration (days) after transplantation. The steatosis grade increased according to the following relationship: $y = 0.0002x^2 + 0.0102x - 0.4416$, where x is days after transplantation, and y is steatosis grade. The correlation coefficient was $r^2 = 0.3455$. The *dashed line* represents the best-fit curve for the above equation.

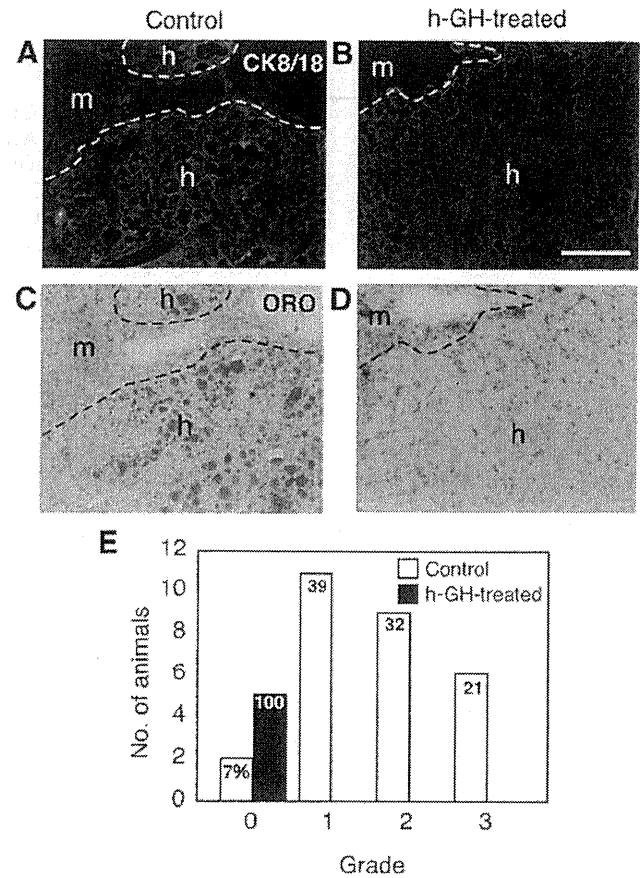

FIG. 2. Effects of h-GH on liver steatosis. Five chimeric mice$_{6YF}$ were given h-GH in the last 2 wk before being killed 70–90 d after transplantation. Twenty-eight of the mice$_{6YF}$ shown in Fig. 1C were killed at 70–90 d as h-GH-untreated animals. A–D, Histology. A control (6YF, no. 1 in Table 2) (A) and h-GH-treated mouse (6YF no. 4 in Table 2) (B) were killed at 97 and 84 d after h-hepatocyte transplantation, respectively, for h-CK8/18 immunohistochemistry to identify h-hepatocytes. Primary antibodies were visualized with Alexa 594-conjugated anti-m-IgG goat sera (Molecular Probes, Eugene, OR). Serial sections from the control (C) and h-GH-treated mouse (D) were stained with ORO. Small to large droplets are diffusely distributed in h-hepatocytes from control chimeric liver (grade 3) but are absent in h-GH-treated animals (grade 0); m and h indicate regions of m- and h-hepatocytes, respectively. *Dotted lines* show the boundary between the two regions. *Bar*, 100 μm. E, Steatosis graded for 28 controls (*white bars*) and five h-GH-treated chimeric mice (*black bar*). *Arabic numerals* in the *bars* represent the percentage in each case (control or h-GH-treated animals). All h-GH-treated chimeric mice were of grade 0.

obtained mRNA expression profiles were referred to as profiles at the hepatocyte level: profiles of h-GH-untreated (n = 3) and h-GH-treated h-hepatocytes$_{\text{chimeric mouse}}$ (n = 3).

Microarray analysis at the liver tissue level

Six chimeric mice$_{6YF}$ [nos. 1–6 (Table 2)] were used for the liver tissue-level assay. Half of six chimeric mice$_{6YF}$ (nos. 4–6) were treated with h-GH, and the other half (nos. 1–3) served as controls. Liver tissues consisted of three visually identifiable regions of different colors. White, red, and medium-colored regions between the white and red regions corresponded to those of original diseased m-hepatocytes, uPA gene-deleted m-hepatocytes, and h-hepatocytes, respectively (1). h-Hepatocyte regions were dissected from livers of chimeric mice$_{6YF}$ using a razor blade for RNA extraction. The obtained mRNA expression profiles were referred to as profiles at the liver tissue level.

Determination of gene expression by real-time qRT-PCR

mRNA expression was determined by real time qRT-PCR in human livers and h-GH-untreated and -treated chimeric mouse livers for h-GH-regulated genes selected from microarray analysis and lipogenesis-related genes (Table 3). Sources for extraction of total RNA are shown in Tables 1 and 2. cDNA was

TABLE 3. Primers

Gene	Forward primers (5′–3′)	Reverse primers (5′–3′)
IGF-I	GCTTCCGGAGCTGTGATCTAA	GCTGACTTGGCAGGCTTG
SOCS2	GCAAGGATAAGCGGACAGG	GCGGTTTGGTCAGATAAAGGT
NNMT	CCGGGAGGCAGTAGAGGC	GTCCTTCGTTGTTGGCCAT
IGFLS	TCTGCAGGGCGAAGTCC	
KLOTHO	AGCCATTATACCACCATCCTTG	GTCGGTCATTTCTTGCACTTCTA
P4AH1	TGGATACCCATTTGTTGCCA	
SLC16A1	TGCTGGAGCCCTCATGC	TTCCAGCTTTCTCAAGGGATG
SRD5A1	TACGTATTCAAATAAGCCTCCCCT	
SCD	TCAAAACAGTGTGTTCGTTGC	CATAAGGACGATATCCGAAGAGG
FADS1	CAGGCCACATGCAATGTC	ATCTAGCCAGAGCTGCCCTG
FADS2	GGCTCTCCAGGAACCTGATG	
FASN	GGCAAATTCGACCTTTCTCAG	AGGACCCCGTGGAATGTC
DGAT2	ACGGCCTTACCTGGCTACA	AGACATCAGGTACTCCCTCAACAC
ADPN	CCTCCAGGTCCCAAATGCC	CCAGTCCTGCTCAGGTGTGC
AKR1B10	GGCCTGTAACGTGTTGC	ATGGGACATGAGTGGAGG
SREBP1c	CATGGATTGCACATTTGAAG	CAGAGAGGAGGCCAGAGAA
FABP	GATCCAAAACGAATTCACGG	ATTGTCACCTTCCAACTGAACC
GAPDH	CCACCTTTGACGACGCTGGG	CATACCAGGAAATGAGCTTGACA

synthesized using 1 μg RNA and PowerScript reverse transcriptase (Clontech, Mountain View, CA) and oligo-deoxythymidine primers (Invitrogen) and was subjected to real-time qRT-PCR following the manufacturer's instructions. Genes were amplified with a set of gene-specific primers (Table 3) and SYBR Green PCR mix in a PRISM 7700 sequence detector (Applied Biosystems, Tokyo, Japan). These primers were capable of amplifying human, but not mouse, genes. PCR products were monitored during amplification. All data were calculated by the comparative threshold cycle (Ct) method (22). Occupancy rates of h-hepatocytes in h-hepatocyte regions ranged from 70–95% (Table 2). Contamination of m-hepatocytes did not affect RT-PCR results of human gene expression because each gene's expression level was normalized against h-*GAPDH*.

Responsiveness of h-hepatocytes$_{\text{chimeric mouse}}$ to h-GH and h-IGF-I

Hepatocytes synthesize and secrete IGF-I when GH receptors are activated by GH (23). To determine whether h-GH directly regulates GH-responsive genes or h-IGF-I, h-hepatocytes$_{6YF}$ (9×10^5 cells) from three chimeric mice were cultured in 1.8-cm Matrigel-coated dishes in DMEM as previously reported (24), and 4 h later, they were exposed with 0, 5, and 50 ng/ml h-GH or 50 and 500 ng/ml h-IGF-I for an additional 24 and 48 h and harvested in RLT buffer to prepare total RNA for real-time qRT-PCR.

Gene enrichment analysis

Gene and gene ontology (GO) information were collected from NCBI build 37.1 (ftp://ftp.ncbi.nlm.nih.gov/gene/DATA/gene2go.gz) and The Gene Ontology (http://www.geneontology.org/ontology/gene_ontology.obo) sites, respectively. Pathway information was collected from KEGG (ftp://ftp.genome.jp/pub/kegg/pathway/organisms/hsa/hsa_gene_map.tab) and Ingenuity Pathways Analysis (IPA) software (Ingenuity Systems, Redwood City, CA). The gene enrichment analysis was performed using only GO and pathway groups where at least two genes or more were assigned.

Statistics

Microarray data were evaluated by the Welch's *t* test (two-sided). The gene enrichment analysis was calculated using Fisher's exact test and corrected with Benjamini-Hochberg's false discovery rate (25). The significance of overlap between two groups of transcripts was determined using Fisher's exact test. Log_{10}-transformed data obtained in real-time qRT-PCR analysis of *in vivo* and *in vitro* studies were analyzed among groups by ANOVA. When the overall F statistics were significant, significance was determined by the Scheffé's test with significance level $\alpha = 0.05$.

Results

Lipid accumulation in chimeric mouse livers

Hepatocytes$_{6YF}$ were transplanted to uPA/SCID mice, and the process of h-hepatocyte repopulation in host livers was visualized using hematoxylin- and eosin-stained histological sections. Vacuoles appeared in the cytoplasm of donor h-hepatocytes approximately 70 d after transplantation and gradually increased in numbers and sizes thereafter (Fig. 1A, a and b). To test whether these vacuoles represent lipid deposits, 36 chimeric mice$_{6YF}$ were killed 48–111 d after transplantation (five before 60 d, 28 between 70 and 90 d, and three after 90 d) for ORO staining of liver sections (Fig. 1B). Most of the chimeric liver h-hepatocytes became ORO$^+$ approximately 70 d after transplantation. The steatosis level was quantified by the size and frequency of ORO$^+$ lipid droplets from grade 0 (Fig. 1Ba) to grade 3 (Fig. 1Bd) and plotted against post-transplantation days (Fig. 1C). Among five livers before 60 d of transplantation, one and four livers were of grade 0 and 1, respectively (Fig. 1C). Most of the livers between 70 and 90 d were of grade 1 (11 of 28 mice) and grade 2

(nine of 28). All three livers after 90 d were of grade 3, showing a good correlation of the steatosis level with post-transplantation duration (~50–110 d). h-IGF-I serum levels of chimeric mice$_{6YF}$, a measure of h-GH level, were under a detection limit of 9.4 ng/ml (n = 3), which supported our previous study that chimeric mouse h-hepatocytes were h-GH deficient (6). Therefore, we considered h-GH deficiency as an etiological factor in the observed hepatic lipogenesis.

Improvement of liver steatosis in chimeric mice by h-GH

To examine the relationship of steatosis with-GH-deficiency, five chimeric mice$_{6YF}$ at different time points after transplantation were infused with h-GH during the last 2 wk before killing (one mouse was killed at 83 d, three at 84 d, and the remaining one at 89 d) and were used as h-GH-treated chimeric mice. Twenty-eight of 36 chimeric mice$_{6YF}$ that were used in the experiment shown in Fig. 1C and killed 70–90 d after transplantation served as controls. The h-IGF-I serum level rose to 72.5 ± 9.4 ng/ml (n = 3) in h-GH-treated mice, a level comparable to that in normal human sera, proving the effectiveness of the h-GH treatment. Serial histological sections were immunostained for h-CK8/18 to identify h-hepatocytes (Fig. 2, A and B) and stained with ORO (Fig. 2, C and D). ORO$^+$ droplets were present in the control mouse h-hepatocytes (Fig. 2, A and C) but were not in h-GH-treated ones (Fig. 2, B and D). Some host m-hepatocytes also contained small cytoplasmic ORO$^+$ droplets (Fig. 2, A and C), probably due to uPA damage because even after h-GH treatment, these lipid droplets remained (Fig. 2, B and D). Steatosis grading on liver sections showed that most of the control mouse livers (93%) were of grade 1–3: 39, 32, and 21% for grades 1, 2, and 3, respectively (Fig. 2E). All h-GH-treated livers were of grade 0. Therefore, we concluded that h-GH plays a critical role in the etiology of human liver steatosis.

h-GH-induced changes in gene expression profiles at the hepatocyte level

Hepatocytes were isolated from three h-GH-untreated chimeric mice$_{9MM}$ 72–101 d after transplantation (nos. 1–3) and three h-GH-treated chimeric mice$_{9MM}$ 75 d after transplantation (nos. 4–6) for microarray analysis (Table 2). We found 15,826 positive transcripts (29%) in 54,675 spotted transcripts in either h-GH-untreated or -treated h-hepatocytes$_{\text{chimeric liver}}$. Among these, 229 (1.4%) and 269 (1.7%) transcripts showed more than 2-fold higher and lower expression levels in h-GH-treated than -untreated h-hepatocytes, respectively. Statistical evaluation at $P < 0.05$ selected 58 genes (82 transcripts) from 229 transcripts as up-regulated in h-GH-treated h-hepatocytes$_{\text{chimeric mouse}}$. Similarly, 33 genes (37 transcripts) were selected from the 269 transcripts as down-regulated genes.

Gene enrichment analysis on transcripts showing more than 2-fold changes selected the significantly overrepresented (GH-induced and -suppressed) GO terms and pathways including GH signaling, IGF-I receptor binding, response to hormone stimulus, lipid biosynthetic process, and aging (Table 4 and Supplemental Table 1, published on The Endocrine Society's Journals Online web site at http://endo.endojournals.org).

TABLE 4. Extracted significantly overrepresented GO terms and pathways

Pathway, or GO term	*P* value	B-H FDR q-value
Hepatocyte level		
Pathway		
GH signaling	0.000244	0.00830
GO molecular function		
IGF receptor binding	3.77×10^{-5}	0.00464
GO biological process		
Response to hormone stimulus	4.30×10^{-5}	0.00556
Lipid biosynthetic process	0.000898	0.0251
Lipid metabolic process	0.00122	0.0284
Aging	0.00288	0.0334
Regulation of fatty acid biosynthetic process	0.00353	0.0358
Regulation of lipid metabolic process	0.0241	0.0947
Tissue level		
Pathway		
Biosynthesis of unsaturated fatty acids	2.78×10^{-5}	0.000584
GH signaling	0.0116	0.0612
GO molecular function		
Stearoyl-coenzyme A 9-desaturase activity	8.78×10^{-5}	0.00382
IGF receptor binding	0.00256	0.0500
GO biological process		
Fatty acid metabolic process	0.000189	0.00585
Lipid metabolic process	0.000739	0.0133
Oxidation reduction	0.00312	0.0288
Response to hormone stimulus	0.00468	0.0346
Aging	0.00627	0.0392
Unsaturated fatty acid biosynthetic process	0.0186	0.0692

B-H FDR, Benjamini-Hochberg's false discovery rate.

h-GH-induced changes in gene expression profiles at the liver tissue level

Identical microarray analysis was performed at the liver tissue level with six chimeric mice$_{6YF}$ (Table 2), with half (nos. 1–3) being used as controls and the other half (nos. 4–6) as h-GH-treated mice. In this analysis, h-hepatocyte-repopulated regions were dissected from liver tissues of these animals and used as h-liver$_{\text{chimeric mouse}}$ as RNA sources for microarray analysis in which 54,675 transcripts were spotted as in the case of the hepatocyte-level analysis. Transcripts positive for either h-GH-untreated or -treated h-liver$_{\text{chimeric mouse}}$ were 18,210 (33%) transcripts, among which 146 (0.8%) and 237 (1.3%) transcripts were expressed at more than 2-fold higher and lower levels, respectively, in h-GH-treated tissues than in h-GH-untreated controls. Through statistical evaluation ($P < 0.05$), we identified 43 genes (64 transcripts) and 55 genes (76 transcripts) as up- and down-regulated genes by h-GH from the 146 and 237 transcripts, respectively.

Gene enrichment analysis on transcripts showing more than 2-fold changes selected the significantly overrepresented (GH-induced and -suppressed) GO terms and pathways including biosynthesis of unsaturated fatty acids, GH signaling, stearoyl-coenzyme A desaturase (SCD) activity, IGF receptor binding, oxidoreductase activity, fatty acid metabolic process, aging were significantly changed (Table 4 and Supplemental Table 2).

In summary, we selected 58 up-regulated and 33 down-regulated genes from the h-hepatocyte-level assay and 43 up-regulated and 55 down-regulated genes from the h-liver tissue-level assay. From them, we chose genes that were commonly up- and down-regulated at both the hepatocyte and liver tissue levels. As a result, 14 up-regulated genes (23 transcripts) and four down-regulated genes (five transcripts) were finally identified as more reliable candidates for h-GH-responsive genes as listed in Table 5, in which the expression ratios at the hepatocyte level [h-GH-treated h-hepatocytes$_{\text{chimeric mouse}}$ *vs.* h-GH-untreated h-

TABLE 5. h-GH-regulated genes

Affymetrix ID	Gene symbol	Accession Number	Gene name	Cell level, treated/untreated		Tissue level, treated/untreated	
				Microarray	RT-PCR[a]	Microarray	RT-PCR[a]
Up-regulated							
209988_s_at	*ASCL1*	NM_004316.3	Achaete-scute complex-like 1	123.39	–	151.42	–
209540_at	*IGF1*[b]	AU144912	IGF-I	179.66	159.83	34.19	35.45
203373_at	*SOCS2*[b]	NM_003877	Suppressor of cytokine signaling 2	39.01	73.79	13.91	53.20
202237_at	*NNMT*[b]	NM_006169	Nicotinamide *N*-methyltransferase	46.02	40.09	14.28	20.79
205978_at	*KL*[b]	NM_004795	Klotho	39.90	22.50	6.58	8.45
207543_s_at	*P4HA1*[b]	NM_000917	Procollagen-proline, 2-oxoglutarate 4-dioxygenase, α-polypeptide I	15.17	11.99	9.69	9.03
203498_at	*DSCR1L1*	NM_005822	Down syndrome critical region gene 1-like 1	5.77	–	4.06	–
215712_s_at	*IGFALS*[b]	AW338791	IGF-binding protein, acid labile subunit	5.29	9.49	7.29	13.63
209967_s_at	*CREM*	D14826	cAMP-responsive element modulator	4.41	–	2.76	–
207256_at	*MBL2*	NM_000242	Mannose-binding lectin 2, soluble	3.44	–	2.09	–
222108_at	*AMIGO2*	AC004010	Adhesion molecule with Ig-like domain 2	2.89	–	2.84	–
201309_x_at	*C5orf13*	U36189	Chromosome 5 open reading frame 13	2.75	–	3.47	–
202234_s_at	*SLC16A1*[b]	BF511091	Solute carrier family 16, member 1	2.74	2.29	4.14	3.84
211056_s_at	*SRD5A1*[b]	BC006373	Steroid-5-α-reductase, α-polypeptide 1	2.29	1.99	2.03	1.72
Down-regulated							
208964_s_at	*FADS1*[b]	AL512760	Fatty acid desaturase 1	0.43	0.51	0.36	0.29
219295_s_at	*PCOLCE2*	NM_013363	Procollagen C-endopeptidase enhancer 2	0.37	–	0.45	–
206561_s_at	*AKR1B10*[b]	NM_020299	Aldo-keto reductase family 1, member B10	0.22	0.22	0.19	0.13
202628_s_at	*SERPINE1*	NM_000602	Serine proteinase inhibitor, clade E, member 1	0.17	–	0.28	–

Treated indicates h-GH-treated chimeric mouse, whereas untreated indicates h-GH-untreated chimeric mouse. –, Not determined.

[a] The expression level of each gene was divided with that of h-*GAPDH*.

[b] Gene expression levels were determined by both microarray assay and real-time qRT-PCR.

hepatocytes$_{\text{chimeric mouse}}$ (cell level, treated/untreated)] and at the tissue level [h-GH-treated h-liver$_{\text{chimeric mouse}}$ *vs.* -untreated h-liver$_{\text{chimeric mouse}}$ (tissue level, treated/untreated)] are presented for each gene. *P* values for overrepresentation of the overlapping genes (up- and down-regulated genes in both hepatocytes and liver tissue levels) were 5.34×10^{-9} and 1.92×10^{-9}, respectively, which indicates the significance of the overlapping.

The microarray assay's results were validated by real-time qRT-PCR using RNA extracted from the sources shown in Table 2 on arbitrarily selected eight and three genes from the above final 14 h-GH-up- and four h-GH-down-regulated genes, respectively: *IGF-I*, suppressor of cytokine signaling 2 (*SOCS2*), nicotinamide *N*-methyltransferase (*NNMT*), *KL*, *P4HA1*, *IGFALS*, solute carrier family 16/member 1 (*SLC16A1*), and steroid-5-α-reductase and α-polypeptide 1 (*SRD5A1*) as h-GH-up-regulated genes and fatty acid desaturase (*FADS1*) and aldo-keto reductase family 1/member B10 (*AKR1B10*) as h-GH-down-regulated genes. The expression ratios (treated/untreated) calculated from the qRT-PCR results are included in Table 5, which well support the microarray data, indicating the reliability of the microarray data.

There was the possibility that mouse transcripts were also included as the cDNAs hybridized in the currently adopted microarray assay. To check this possibility, pooled cDNAs of three uPA/SCID mouse livers were subjected to the microarray with 54,675 cDNA spots, which gave a result that 5,643 of 54,675 transcripts (10.3%) were positive. Sixteen genes among the genes listed in Table 5 were not found in these positive genes, but two genes, *SOCS2* and *IGFALS*, both h-GH-up-regulated genes, were found there. Considering that the cross-hybridized signals were less than 10% of those in the GH-untreated hepatocytes$_{\text{chimeric mouse}}$ and the contamination of mouse hepatocytes in the h-hepatocyte preparation used in the present study was less than 10% (Table 2, 9MM nos. 1–6), we concluded that their ratios of treated to untreated genes were high enough to include them as h-GH-regulated genes in the present study. This conclusion was further validated by measuring m-Alb mRNA expression levels in the h-liver$_{\text{chimeric mouse}}$. Real-time qRT-PCR was performed for RNAs isolated from h-liver$_{\text{chimeric mouse}}$ (Table 2, 6YF nos. 1–6) using a set of m-Alb primers. The result showed that m-Alb expression levels in the h-liver$_{\text{chimeric mouse}}$ were 0.5 ± 0.2% of those of the uPA/SCID mouse liver. As a whole, it can be said that the cross-reactivity does not affect the results in the present study.

Improvement of gene expression by h-GH

Real-time qRT-PCR was performed for livers of h-GH-untreated chimeric, h-GH-treated chimeric mice, and humans, the last of which accurately reflect the physiology of h-GH endocrine regulation. The h-GH-untreated and -treated h-hepatocytes$_{\text{chimeric mouse}}$ were isolated from nos. 1–3 and nos. 4–6 of chimeric mice$_{\text{9MM}}$, respectively (Table 2). The h-GH-untreated and -treated h-liver$_{\text{chimeric mouse}}$ were isolated from nos. 1–3 and nos. 4–6 of chimeric mice$_{\text{6YF}}$, respectively (Table 2). The h-hepatocytes$_{\text{human}}$ and h-liver$_{\text{human}}$ were isolated from four (28YM, 57YM, 25YF, and 61YF) and three (28YM, 25YF, and 61YF) donors, respectively (Table 1). Expression levels in h-hepatocytes$_{\text{chimeric mouse}}$ and h-liver$_{\text{chimeric mouse}}$ under h-GH-untreated and -treated conditions were divided by the h-hepatocyte$_{\text{human}}$ and the h-liver$_{\text{human}}$, respectively, which is shown as the hepatocyte ratio (*white bars*) and liver-tissue ratio (*black bars*), respectively (Fig. 3). The ratios are used as measures of the extent of difference/closeness of the gene expression level in h-GH-treated or -untreated chimeric livers from/to that in human liver. If h-GH improves gene expressions in chimeric mouse livers, ratios for h-GH-up-regulated genes in h-GH-untreated and -treated chimeric liver are expected to be less than 1 and approximately 1, respectively, and ratios for h-GH-down-regulated genes in h-GH-untreated and -treated chimeric liver are expected to be more than 1 and approximately 1, respectively.

Expression levels of a total of eight h-GH-up-regulated genes were compared between h-GH-untreated and -treated chimeric mice at both hepatocyte and liver tissue levels. The results of the h-GH-up-regulated genes are shown in Fig. 3A. Generally, the expressions of the genes, except *KL*, were significantly suppressed in the absence of h-GH at both the hepatocyte and liver tissue levels. Expression in h-GH-treated cases was similar to that in human livers: *IGF-I* and *P4AH1* at the tissue level and *IGFALS* and *SLC16A1* at both levels. *KL* expression in h-GH-untreated chimeric mice was similar to that in human livers at both levels, and h-GH treatment markedly increased expression over that in human livers at both levels, suggesting that its expression is greatly up-regulated by GH. *In vivo*, h-GH-up-regulated genes of human livers are likely positively induced by GH.

Our results on suppression of spontaneous lipogenesis by GH (Fig. 2) and a reported relationship between GH-responsive genes and lipogenesis-related genes (26) suggest an association between the h-GH-responsive genes listed in Table 5 and the observed hepatic lipogenesis. Gene enrichment analysis showed that h-GH-responsive genes were enriched as those involved in the lipid synthesis process, lipid metabolic process, and regulation of fatty acid biosynthetic process (Table 4). Of the two down-regulated genes, *FADS1* is known to be lipogenesis related (27), and *AKR1B10* was recently reported to regulate fatty acid synthesis (28). Five genes were additionally cho-

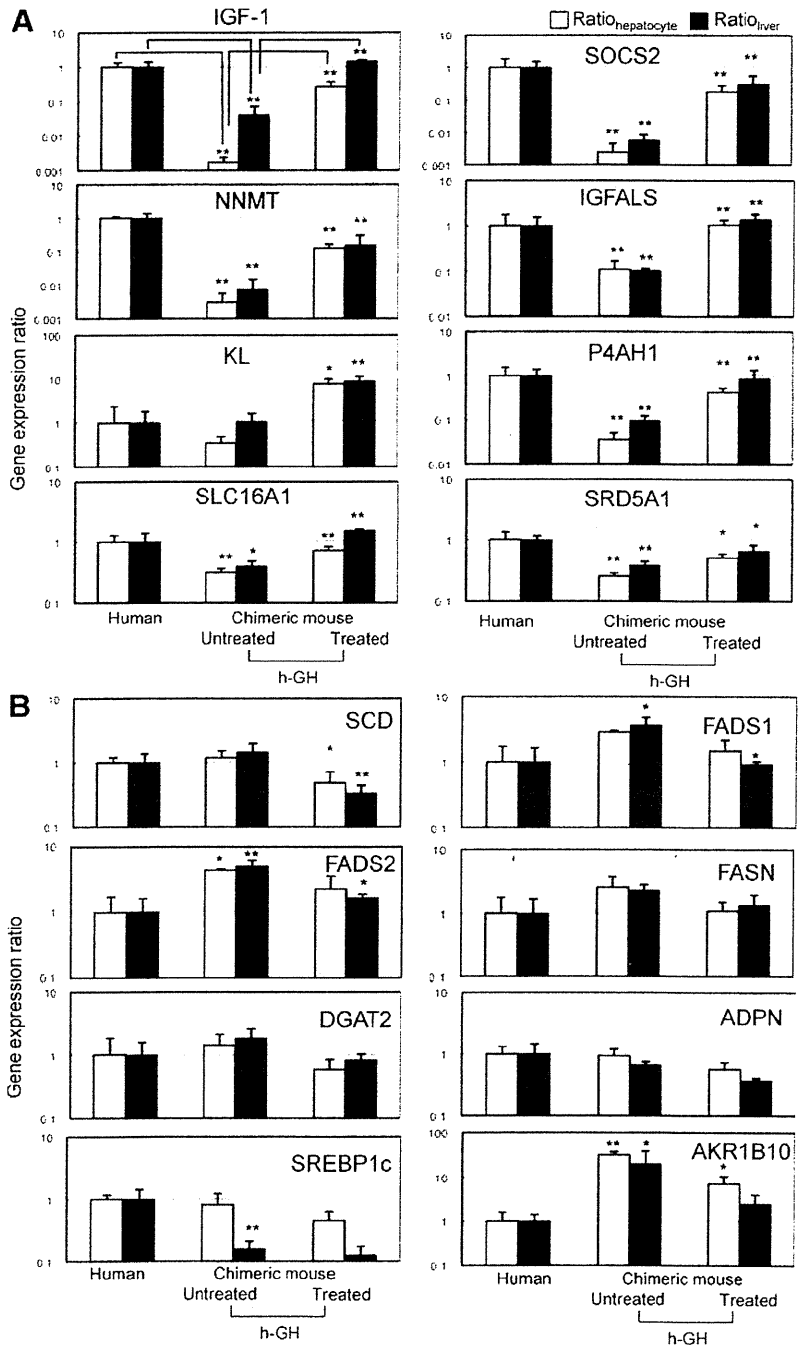

FIG. 3. Regulation of gene expression in h-hepatocytes$_{\text{chimeric mouse}}$ by h-GH at the hepatocyte and liver tissue levels. Six chimeric mice$_{9MM}$ and six chimeric mice$_{6YF}$ were produced (Table 2); half of each group (nos. 1–3 for both the chimeric mice$_{9MM}$ and chimeric mice$_{6YF}$) served as control animals, and the remaining half (nos. 4–6 for both the chimeric mice$_{9MM}$ and chimeric mice$_{6YF}$) were treated with h-GH. h-Hepatocytes$_{\text{chimeric mouse}}$ and h-livers$_{\text{chimeric mouse}}$ were isolated from the former and latter chimeric mice, respectively. h-Hepatocytes$_{\text{human}}$ and h-livers$_{\text{human}}$ were also isolated from four (25YF, 28YM, 57YM, and 61YF) and three (25YF, 28YM and 61YF) human donors, respectively (Table 1). RNA was isolated from the hepatocytes and liver tissue for real-time qRT-PCR analysis. qRT-PCR was performed for eight h-GH-up-regulated (A) and eight lipogenesis-related (B) genes. The expression level of each gene was normalized against that of h-*GAPDH*. The expression level of h-GH-untreated h-hepatocytes$_{\text{chimeric mouse}}$ and h-GH-treated h-hepatocytes$_{\text{chimeric mouse}}$ was divided by that of h-hepatocytes$_{\text{human}}$ (ratio$_{\text{hepatocyte}}$). Similarly, the expression level of h-livers$_{\text{chimeric mouse}}$ was divided by that of h-livers$_{\text{human}}$ (ratio$_{\text{liver}}$). *White* and *black bars* represent the ratio$_{\text{hepatocyte}}$ and the ratio$_{\text{liver}}$, respectively. Each value represents the mean ± SD. *Asterisks above bars* of untreated chimeric mouse show significance between human and GH-untreated chimeric mouse. *Asterisks above bars* of treated chimeric mouse show significance between human and GH-treated chimeric mouse. *, $P < 0.05$; **, $P < 0.01$.

sen to examine the relationship between h-GH-down-regulated genes and known lipogenic genes from previous studies: *FADS2* (27), *SCD* (29), *FASN* (30), diacylglycerol acyltransferase 2 gene (*DGAT2*) (31), and the adiponutrin gene [*ADPN* (32), currently known as *PNPLA3* (33)]. These genes were included as h-GH-down-regulated genes at either the hepatocyte or liver tissue level in the microarray assay; *FADS2* and *SCD* were significantly ($P < 0.05$) down-regulated only at the liver tissue level, *FASN* was insignificantly (>2-fold) down-regulated only at the hepatocyte level, *DGAT2* was insignificantly (>2-fold) down-regulated only at the hepatocyte level, and *ADPN* significantly ($P < 0.05$) decreased its expression only at the hepatocyte level. Two known GH-inducible lipogenesis-related genes, *SREBP1c* (34–36) and fatty acid-binding protein gene (*FABP*) (24, 37), were also chosen from previous studies.

Expression of a total of nine genes was compared between human livers and h-GH-untreated and -treated chimeric mice at both hepatocyte and liver tissue levels as above. Results for lipogenesis-related genes are shown in Fig. 3B. Ratios of three genes, *FADS1* (significant at tissue level), *FADS2* (significant at both levels), and *AKR1B10* (significant at both levels), were higher in the h-GH-untreated chimeric mice compared with humans, and h-GH treatment lowered the ratios of *SCD* (significant at both levels), *FADS1* (significant at tissue level), *FADS2* (significant at tissue level), and *AKR1B10* (significant at hepatocyte level). Although not significantly, ratios of *FASN* and *DGAT2* were also higher in the h-GH-untreated chimeric mice compared with humans and decreased by h-GH treatment. *ADPN* expression in h-GH-untreated chimeric mice was close to that in humans at both levels, and h-GH treatment decreased ratios (insignificant). Thus, it is most likely that these lipogenesis-related genes are down-regulated by h-GH. Ratios of *SREBP1c* (Fig.

3B) and *FABP* (data not shown) genes did not show any meaningful changes by h-GH at either the hepatocyte or liver tissue level under the observed endocrinological conditions, although *SREBP1* expression was significantly lower at tissue levels in h-GH-untreated chimeric mice compared with human.

Deletion of GH receptor gene (*GHR*) in mice resulted in an increase of insulin receptor gene (*IRS*) expression (38) and a reduction of plasma levels of IGF-I, insulin, and glucose, implying that the mice increased insulin sensitivity (39, 40). These studies suggested the possibility that chimeric mice are insulin sensitive. Thus, we examined whether chimeric mice are insulin sensitive by determining the expression levels of h-*GHR* and h-*IRS*. Real-time qRT-PCR analysis showed that h-*GHR* and h-*IRS* expression levels in chimeric mice were similar or higher than humans, and h-GH administration of chimeric mice did not affect these observed expression levels. However chimeric mice did not show any sign of insulin resistance or sensitivity in a sugar tolerance test (data not shown). As a whole, we currently consider that chimeric mice are not insulin sensitive.

In vitro effects of h-GH on gene expressions in h-hepatocytes

We asked whether the aforementioned effects of h-GH on the h-GH-up-regulated gene and lipogenic gene expression in chimeric mouse livers *in vivo* are reproducible *in vitro*. h-Hepatocytes$_{6YF}$ isolated from three chimeric mice with RI_{Alb} higher than 95% at 70–80 d after transplantation were cultured for 24 and 48 h in the presence and absence of h-GH and h-IGF-I, followed by determination of expression levels of the eight h-GH-up-regulated genes by real-time qRT-PCR (Fig. 4A). Expression of *IGF-I*, *SOCS2*, *NNMT*, *IGFALS*, and *P4AH1* were significantly increased by h-GH in a dose-dependent manner, but h-IGF-I did not enhance expression of the genes, indicating the direct the action of h-GH on the expression of these genes. The remaining three genes (*KL*, *SLC16A1*, and *SRD5A1*) were not responsive to h-GH or h-IGF-I.

Results for lipogenic genes (*SCD*, *FADS1*, *FADS2*, *FASN*, *DGAT2*, *ADPN*, *AKR1B10*, and *SREBP1c*) are shown in Fig. 4B. Only *FADS1*, *DGAT2*, *SREBP1c*, and *AKR1B10* significantly decreased the expression at 24 or 48 h exposure of 50 ng/ml h-GH. Although insignificant, *SCD*, *FADS2*, and *FASN* were decreased by GH exposure. The expression levels of the eight genes did not significantly change by h-IGF-I.

Discussion

GH regulation of lipogenic genes has been generally studied using rodents (34–37, 41–43), and no suitable animal model whose liver mimics the human liver has been available. Currently, we propose an h-hepatocyte-bearing chimeric mouse as one such model, in which heavy lipid accumulation spontaneously takes place in h-hepatocytes more than 2 months after transplantation but does not when the animals are administered h-GH. Using this model, we demonstrated that h-GH deficiency is a cause of the steatosis and identified 14 and four genes as h-GH-up- and -down-regulated genes at both the hepatocyte and liver tissue level, in which three new lipogenic genes (*FADS1*, *FADS2*, and *AKR1B10*) were included. Regarding h-GH-down-regulated genes, we characterized an additional seven lipogenic genes, although these genes were h-GH down-regulated only at the hepatocyte level or liver tissue level. *FADS1*, *FADS2*, and *AKR1B10* were included in these seven genes and were significantly up-regulated in the chimeric mouse liver compared with human liver, but their expression was down-regulated by h-GH. Thus, it is suggested that these genes participate in the spontaneous steatosis observed in the chimeric mouse liver.

Results of previous studies indicated the presence of species differences in GH responsiveness of lipogenic genes between rats and mice. *SREBP-1c*, a known transcription factor of lipogenic genes, and its target genes, *FASN* and *SCD-1*, appear to be GH up-regulated in rats; hypophysectomy decreases expression of these genes, and the infusion of the rats with GH improved their expression to the original levels (34, 35). By contrast, a study with GH-transgenic technology showed that the same genes were down-regulated in mice (44). Recent microarray analysis supported such species differences; GH treatment suppressed *SCD* gene expression level in hypophysectomized mouse livers (42) but not in hypophysectomized rat livers (41). There are also differences regarding GH responsiveness of lipogenic genes between *in vitro* and *in vivo* studies; the above cited authors showed in a study with primary cultures of rat hepatocytes *SCD1* as GH up-regulated, *FASN* as GH down-regulated, and *SREBP-1c* as GH nonresponsive (34). In the present study, expression of h-*SCD*, but not h-*SREBP-1c*, was reduced by h-GH administration to the chimeric mice, and h-*FABP* expression was not affected by h-GH, which was different from a rat study (34). h-*FADS1*, h-*FADS2*, and h-*AKR1B10* were down-regulated in the present study, but they did not report them as GH-down-regulated genes in rodent studies. In addition, AGHD patients show fatty liver and nonalcoholic steatohepatitis (NASH) (8), and GH treatment improved the symptoms (13, 14). However, studies using hypophysectomized rodents did not report such changes (34, 35, 41, 42).

The serum concentration of GH is low in nonalcoholic fatty liver disease (NAFLD) patients (15), and *NNMT* and

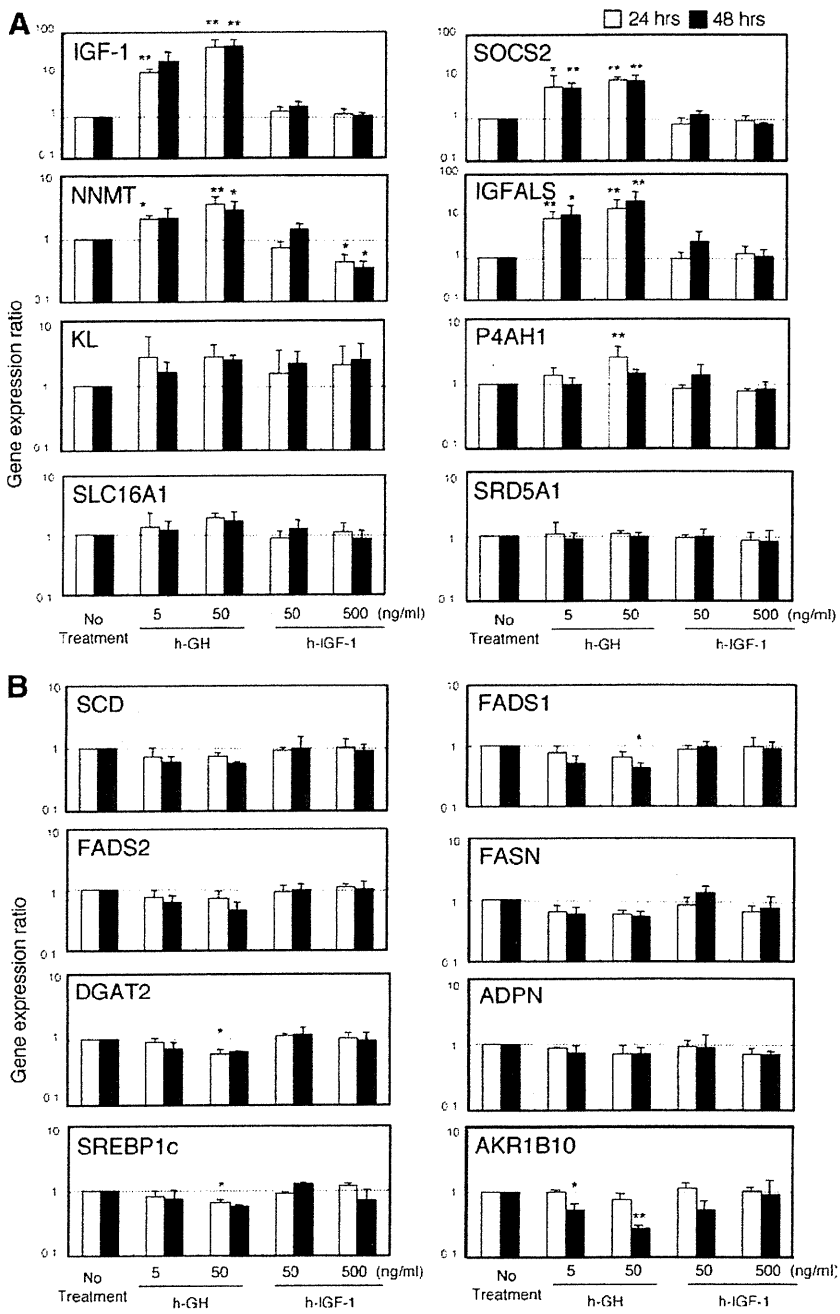

FIG. 4. *In vitro* effects of h-GH and h-IGF-I on the expression level of lipogenesis genes. h-Hepatocytes$_{6YF}$ were cultured with 0, 5, or 50 ng/ml h-GH or 50 or 500 ng/ml h-IGF-I for 24 and 48 h and subjected to RNA isolation to perform real-time qRT-PCR analysis for eight h-GH-up-regulated genes (A) and eight lipogenesis-related genes (B). The expression level of each gene was normalized against that of h-*GAPDH*. The gene expression level of h-hepatocytes treated with h-GH or h-IGF-I was divided by that of untreated h-hepatocytes. *White* and *black bars* represent 24 and 48 h, respectively. Each value represents the mean ± SD. *Asterisks above a bar* show significance between no treatment and each dose of h-GH or h-IGF-I treatment. *, $P < 0.05$; **, $P < 0.01$.

IGFALS are up-regulated in NASH patients (47). Fatty livers of chimeric mice in the present study appreciably reproduce expression profiles of these known NAFLD/NASH-associated genes. We showed that h-GH regulates h-*SCD* and other lipogenesis-related genes, including h-*FADS1*, h-*FADS2*, and h-*AKR1B10* in a h-*SREBP1*-independent manner. Thus, chimeric mice could be particularly useful as an NAFLD/NASH mouse model, with the genes identified in this study serving as therapeutic target genes for NAFLD patients.

Among 14 h-GH-up-regulated genes characterized in this study, eight genes (*IGF-I*, *SOCS2*, *NNMT*, *P4HA1*, *IGFALS*, *MBL2 AMIGO2*, and *SRD5A1*) are known GH-up-regulated genes (23, 41–43, 45), but the remaining six h-GH-up-regulated genes (*ASCL1*, *KL*, *DSCR1L1*, *CREM*, *C5orf13*, and *SLC16A1*) have never been reported as up-regulated genes. Roles of these newly identified GH-up-regulated genes in the human liver could be further investigated using the chimeric mice.

The protein Klotho is known to inhibit insulin/IGF-I signaling, which likely increases resistance to oxidative stress and potentially contributes to its claimed anti-aging properties (46). In the present study, *KL* expression levels were similar in human and chimeric mouse livers, but h-GH markedly induced *KL* gene expression in the latter. The findings of the present study suggested a mutual regulatory mechanism(s) between the two genes: *h-GH* might play a role in the anti-aging process through the *KL* induction.

We were able to propagate h-hepatocytes in chimeric mouse livers, which could solve the problem of a quite limited availability of human hepatocytes for research purposes. In fact, in the present study, we showed the usefulness of chimeric mouse-derived h-hepatocytes for *in vitro* study by testing the effects of h-GH or h-IGF-I on expression levels of eight lipogenic genes that had been up-regulated in chimeric mouse liver *in vivo*. We were able to answer a question of whether h-GH and h-IGF-I in combination directly or indirectly induce such changes in gene expression. Hepatocytes in conventional two-dimensional culture do not generally recapitulate gene expression profiles observed under *in vivo* conditions. In the present study, hepatocytes were three-

dimensionally cultured on Matrigel (spheroid culture), which allowed them to express gene expression closer to *in vivo* conditions as reported previously (48).

We resected h-hepatocyte regions from chimeric livers for microarray analysis and real-time RT-PCR. The gene expression profiles determined using the dissected regions were similar to those determined using the isolated h-hepatocytes$_{\text{chimeric mouse}}$. This finding also indicates the usability of chimeric mouse liver tissues as an alternative RNA source to h-hepatocytes, whose isolation is time consuming and laborious.

In conclusion, the present study shows that chimeric mice could overcome the species difference between experimental animals and humans, and therefore, these mice are useful for investigating the mechanism of the action of GH on h-hepatocytes *in vivo* and role of GH in NAFLD/NASH.

Acknowledgments

We thank Y. Yoshizane, H. Kohno, Y. Matsumoto, and S. Nagai for their technical assistance.

Address all correspondence and requests for reprints to: Katsutoshi Yoshizato, Ph.D., or Chise Tateno, Ph.D., PhoenixBio. Co. Ltd., 3-4-1 Kagamiyama, Higashihiroshima, Hiroshima 739-0046, Japan. E-mail: katsutoshi.yoshizato@phoenixbio.co.jp or chise.mukaidani@phoenixbio.co.jp.

This work was supported by the Yoshizato Project, Cooperative Link of Unique Science and Technology for Economy Revitalization (CLUSTER), Japan.

Disclosure Summary: The authors have no conflicts of interest to disclose.

References

1. Tateno C, Yoshizane Y, Saito N, Kataoka M, Utoh R, Yamasaki C, Tachibana A, Soeno Y, Asahina K, Hino H, Asahara T, Yokoi T, Furukawa T, Yoshizato K 2004 Near-completely humanized liver in mice shows human-type metabolic responses to drugs. Am J Pathol 165:901–912
2. Yoshizato K, Tateno C 2009 A human hepatocyte-bearing mouse: an animal model to predict drug metabolism and effectiveness in humans. PPAR Res 2009:476217
3. Yoshizato K, Tateno C 2009 In vivo modeling of human liver for pharmacological study using humanized mouse. Expert Opin Drug Metab Toxicol 5:1435–1446
4. Katoh M, Matsui T, Okumura H, Nakajima M, Nishimura M, Naito S, Tateno C, Yoshizato K, Yokoi T 2005 Expression of human phase II enzymes in chimeric mice with humanized liver. Drug Metab Dispos 33:1333–1340
5. Nishimura M, Yoshitsugu H, Yokoi T, Tateno C, Kataoka M, Horie T, Yoshizato K, Naito S 2005 Evaluation of mRNA expression of human drug-metabolizing enzymes and transporters in chimeric mouse with humanized liver. Xenobiotica 35:877–890
6. Masumoto N, Tateno C, Tachibana A, Utoh R, Morikawa Y, Shimada T, Momisako H, Itamoto T, Asahara T, Yoshizato K 2007 GH enhances proliferation of human hepatocytes grafted into immunodeficient mice with damaged liver. J Endocrinol 194:529–537
7. Souza SC, Frick GP, Wang X, Kopchick JJ, Lobo RB, Goodman HM 1995 A single arginine residue determines species specificity of the human growth hormone receptor. Proc Natl Acad Sci USA 92:959–963
8. Brunt EM 2010 Pathology of nonalcoholic fatty liver disease. Nat Rev Gastroenterol Hepatol 7:195–203
9. Johannsson G, Bengtsson BA 1999 Growth hormone and the metabolic syndrome. J Endocrinol Invest 22:41–46
10. Ichikawa T, Nakao K, Hamasaki K, Furukawa R, Tsuruta S, Ueda Y, Taura N, Shibata H, Fujimoto M, Toriyama K, Eguchi K 2007 Role of growth hormone, insulin-like growth factor 1 and insulin-like growth factor-binding protein 3 in development of non-alcoholic fatty liver disease. Hepatol Int 1:287–294
11. Ichikawa T, Hamasaki K, Ishikawa H, Ejima E, Eguchi K 2003 Non-alcoholic steatohepatitis and hepatic steatosis in patients with adult onset growth hormone deficiency. Gut 52:914
12. Adams LA, Feldstein A, Lindor KD, Angulo P 2004 Nonalcoholic fatty liver disease among patients with hypothalamic and pituitary dysfunction. Hepatology 39:909–914
13. Takahashi Y, Iida K, Takahashi K, Yoshioka S, Fukuoka H, Takeno R, Imanaka M, Nishizawa H, Takahashi M, Seo Y, Hayashi Y, Kondo T, Okimura Y, Kaji H, Kitazawa R, Kitazawa S, Chihara K 2007 Growth hormone reverses nonalcoholic steaotohepatitis in patients with adult growth hormone deficiency. Gastroenterology 132:938–943
14. Lonardo A, Carani C, Carulli N, Loria P 2006 'Endocrine NAFLD' a hormonocentric perspective of nonalcoholic fatty liver disease pathogenesis. J Hepatol 44:1196–1207
15. Lonardo A, Loria P, Leonardi F, Ganazzi D, Carulli N 2002 Growth hormone plasma levels in nonalcoholic fatty liver disease. Am J Gastroenterol 97:1071–1072
16. Meuleman P, Vanlandschoot P, Leroux-Roels G 2003 A simple and rapid method to determine the zygosity of uPA-transgenic SCID mice. Biochem Biophys Res Commun 308:375–378
17. Jeschke MG, Herndon DN, Finnerty CC, Bolder U, Thompson JC, Mueller U, Wolf SE, Przkora R 2005 The effect of growth hormone on gut mucosal homeostasis and cellular mediators after severe trauma. J Surg Res 127:183–189
18. Utoh R, Tateno C, Yamasaki C, Hiraga N, Kataoka M, Shimada T, Chayama K, Yoshizato K 2008 Susceptibility of chimeric mice with livers repopulated by serially subcultured human hepatocytes to hepatitis B virus. Hepatology 47:435–446
19. Utoh R, Tateno C, Kataoka M, Tachibana A, Masumoto N, Yamasaki C, Shimada T, Itamoto T, Asahara T, Yoshizato K 2010 Hepatic hyperplasia associated with discordant xenogeneic parenchymal-nonparenchymal interactions in human hepatocyte-repopulated mice. Am J Pathol 177:654–665
20. Tateno C, Takai-Kajihara K, Yamasaki C, Sato H, Yoshizato K 2000 Heterogeneity of growth potential of adult rat hepatocytes in vitro. Hepatology 31:65–74
21. Igarashi Y, Tateno C, Tanaka Y, Tachibana A, Utoh R, Kataoka M, Ohdan H, Asahara T, Yoshizato K 2008 Engraftment of human hepatocytes in the livers of rats reconstructed with bone marrow cells from an immunodeficient mouse. Xenotransplantation 15:235–245
22. Asahina K, Sato H, Yamasaki C, Kataoka M, Shiokawa M, Katayama S, Tateno C, Yoshizato K 2002 Pleiotrophin/HB-GAM as a mitogen of rat hepatocytes and its role in regeneration and development of liver. Am J Pathol 160:2191–2205
23. Gosteli-Peter MA, Winterhalter KH, Schmid C, Froesch ER, Zapf J 1994 Expression and regulation of insulin-like growth factor (IGF-I) and IGF-binding protein messenger ribonucleic acid levels in tissues and hypophysectomized rats infused with-IGF-I and growth hormone. Endocrinology 135:2558–2567
24. Thissen JP, Pucilowska JB, Underwood LE 1994 Differential reg-

ulation of insulin-like growth factor I (IGF-I) and IGF binding protein-1 messenger ribonucleic acids by amino acid availability and growth hormone in rat hepatocyte primary culture. Endocrinology 134:1570–1576
25. **Benjamini Y, Hochberg Y** 1995 Controlling the false discovery rate: a practical and powerful approach to multiple testing. J Roy Stat Soc Ser B 57:289–300
26. **Ståhlberg N, Merino R, Hernández LH, Fernández-Pérez L, Sandelin A, Engström P, Tollet-Egnell P, Lenhard B, Flores-Morales A** 2005 A Exploring hepatic hormone actions using a compilation of gene expression profiles. BMC Physiol 5:8
27. **Glaser C, Heinrich J, Koletzko B** 2010 Role of FADS1 and FADS2 polymorphisms in polyunsaturated fatty acid metabolism. Metabolism 59:993–999
28. **Ma J, Yan R, Zu X, Cheng JM, Rao K, Liao DF, Cao D** 2008 Aldo-keto reductase family 1 B10 affects fatty acid synthesis by regulating the stability of acetyl-CoA carboxylase-α in breast cancer cells. J Biol Chem 283:3418–3423
29. **Ntambi JM** 1992 Dietary regulation of stearoyl-CoA desaturase 1 gene expression in mouse liver. J Biol Chem 267:10925–10930
30. **Menendez JA, Lupu R** 2007 Fatty acid synthase and the lipogenic phenotype in cancer pathogenesis. Nat Rev Cancer 7:763–777
31. **Choi CS, Savage DB, Kulkarni A, Yu XX, Liu ZX, Morino K, Kim S, Distefano A, Samuel VT, Neschen S, Zhang D, Wang A, Zhang XM, Kahn M, Cline GW, Pandey SK, Geisler JG, Bhanot S, Monia BP, Shulman GI** 2007 Suppression of diacylglycerol acyltransferase-2 (DGAT2), but not DGAT1, with antisense oligonucleotides reverses diet-induced hepatic steatosis and insulin resistance. J Biol Chem 282:22678–22688
32. **Baulande S, Lasnier F, Lucas M, Pairault J** 2001 Adiponutrin, a transmembrane protein corresponding to a novel dietary- and obesity-linked mRNA specifically expressed in the adipose lineage. J Biol Chem 276:33336–33344
33. **Huang Y, He S, Li JZ, Seo YK, Osborne TF, Cohen JC, Hobbs HH** 2010 A feed-forward loop amplifies nutritional regulation of PNPLA3. Proc Natl Acad Sci USA 107:7892–7897
34. **Améen C, Lindén D, Larsson BM, Mode A, Holmäng A, Oscarsson J** 2004 Effects of gender and GH secretory pattern on sterol regulatory element-binding protein-1c and its target genes in rat liver. Am J Physiol Endocrinol Metab 287:E1039–E1048
35. **Frick F, Lindén D, Améen C, Edén S, Mode A, Oscarsson J** 2002 Interaction between growth hormone and insulin in the regulation of lipoprotein metabolism in the rat. Am J Physiol Endocrinol Metab 283:E1023–E1031
36. **Shimano H, Yahagi N, Amemiya-Kudo M, Hasty AH, Osuga J, Tamura Y, Shionoiri F, Iizuka Y, Ohashi K, Harada K, Gotoda T, Ishibashi S, Yamada N** 1999 Sterol regulatory element-binding protein-1 as a key transcription factor for nutritional induction of lipogeneic enzyme genes. J Biol Chem 274:35832–35839
37. **Carlsson L, Nilsson I, Oscarsson J** 1998 Hormonal regulation of liver fatty acid-binding protein *in vivo* and *in vitro*: effects of growth hormone and insulin. Endocrinology 139:2699–2709
38. **Panici JA, Wang F, Bonkowski MS, Spong A, Bartke A, Pawlikowska L, Kwok PY, Masternak MM** 2009 Is altered expression of hepatic insulin-related genes in growth hormone receptor knockout mice due to GH resistance or a difference in biological life spans? J Gerontol A Biol Sci Med Sci. 2009 64:1126–1133
39. **Liu JL, Coschigano KT, Robertson K, Lipsett M, Guo Y, Kopchick JJ, Kumar U, Liu YL** 2004 Disruption of growth hormone receptor gene causes diminished pancreatic islet size and increased insulin sensitivity in mice. Am J Physiol Endocrinol Metab 287:E405–E413
40. **Dominici FP, Arostegui Diaz G, Bartke A, Kopchick JJ, Turyn D** 2000 Compensatory alterations of insulin signal transduction in liver of growth hormone receptor knockout mice. J Endocrinol 166: 579–590
41. **Wauthier V, Waxman DJ** 2008 Sex-specific early growth hormone response genes in rat liver. Molecular Endocrinology 22:1962–1974
42. **Wauthier V, Sugathan A, Meyer RD, Dombkowski AA, Waxman DJ** 2010 Division of cell and molecular biology intrinsic sex differences in the early growth hormone responsiveness of sex-specific genes in mouse liver. Mol Endocrinol 24:667–678
43. **Tollet-Egnell P, Flores-Morales A, Stavréus-Evers A, Sahlin L, Norstedt G** 1999 Growth hormone regulation of SOCS-2, SOCS-3, and CIS messenger ribonucleic acid expression in the rat. Endocrinology 140:3693–3704
44. **Olsson B, Bohlooly-Y M, Brusehed O, Isaksson OG, Ahrén B, Olofsson SO, Oscarsson J, Törnell J** 2003 Bovine growth hormone-transgenic mice have major alterations in hepatic expression of metabolic genes. Am J Physiol Endocrinol Metab 285:E504–E511
45. **Hansen TK, Thiel S, Dall R, Rosenfalck AM, Trainer P, Flyvbjerg A, Jørgensen JO, Christiansen JS** 2001 GH strongly affects serum concentrations of mannan-binding lectin: evidence for a new IGF-I independent immunomodulatory effect of GH. J Clin Endocrinol Metab 86:5383–5388
46. **Yamamoto M, Clark JD, Pastor JV, Gurnani P, Nandi A, Kurosu H, Miyoshi M, Ogawa Y, Castrillon DH, Rosenblatt KP, Kuro-o M** 2005 Regulation of oxidative stress by the anti-aging hormone klotho. J Biol Chem 280:38029–38034
47. **Younossi ZM, Gorreta F, Ong JP, Schlauch K, Del Giacco L, Elariny H, Van Meter A, Younoszai A, Goodman Z, Baranova A, Christensen A, Grant G, Chandhoke V** 2005 Hepatic gene expression in patients with obesity-related non-alcoholic steatohepatitis. Liver Int 25:760–771
48. **Schuetz EG, Li D, Omiecinski CJ, Muller-Eberhard U, Kleinman HK, Elswick B, Guzelian PS** 1988 Regulation of gene expression in adult rat hepatocytes cultured on a basement membrane matrix. J Cell Physiol 134:309–323

Research Article

EASL EUROPEAN ASSOCIATION FOR THE STUDY OF THE LIVER | JOURNAL OF HEPATOLOGY

ME3738 enhances the effect of interferon and inhibits hepatitis C virus replication both *in vitro* and *in vivo*

Hiromi Abe[1,3], Michio Imamura[1,2], Nobuhiko Hiraga[1,2], Masataka Tsuge[1,2], Fukiko Mitsui[1,2], Tomokazu Kawaoka[1,2], Shoichi Takahashi[1,2], Hidenori Ochi[2,3], Toshiro Maekawa[3], C. Nelson Hayes[1,3], Chise Tateno[2,4], Katsutoshi Yoshizato[2,4], Shoichi Murakami[5], Nobuyuki Yamashita[5], Takashi Matsuhira[5], Kenji Asai[5], Kazuaki Chayama[1,2,3,*]

[1]*Department of Medicine and Molecular Science, Division of Frontier Medical Science, Programs for Biomedical Research, Graduate School of Biomedical Sciences, Hiroshima University, 1-2-3 Kasumi, Minami-ku, Hiroshima-shi 734-8551, Japan;* [2]*Liver Research Project Center, Hiroshima University, Hiroshima, Japan;* [3]*Laboratory for Digestive Diseases, Center for Genomic Medicine, The Institute of Physical and Chemical Research (RIKEN), Hiroshima, Japan;* [4]*PhoenixBio Co., Ltd., Higashihiroshima, Japan;* [5]*Pharmaceutical Research Center, Meiji Seika Kaisha Ltd., Yokohama, Japan*

Background & Aims: ME3738 (22β-methoxyolean-12-ene-3β, 24-diol), a derivative of soyasapogenol B, attenuates liver disease in several animal models of acute and chronic liver injury. ME3738 is thought to inhibit replication of hepatitis C virus (HCV) by enhancing interferon (IFN)-β production, as determined using the HCV full-length binary expression system. We examined the effect of ME3738 combined with IFN-α on HCV replication using the genotype 1b subgenomic replicon system and an *in vivo* mouse HCV model.

Methods: HCV replicon cells (ORN/3-5B/KE cells and Con1 cells) were incubated with ME3738 and/or IFN-α, and then intracellular IFN-stimulated genes (ISGs) and HCV RNA replication were analyzed by reverse-transcription-real time polymerase chain reaction and luciferase reporter assay. HCV-infected human hepatocyte chimeric mice were also treated with ME3738 and/or IFN-α for 4 weeks. Mouse serum HCV RNA titer, HCV core antigen, and ISGs expression in the liver were measured.

Results: ME3738 induced gene expression of oligoadenylate synthetase 1 and inhibited HCV replication in both HCV replicon cells. The drug enhanced the effect of IFN to significantly increase ISG expression levels, inhibit HCV replication in replicon cells, and reduce mouse serum HCV RNA and core antigen levels in mouse livers. The combination treatment was not hepatotoxic as evident histologically and did not reduce human serum albumin in mice.

Conclusions: ME3738 inhibited HCV replication, enhancing the effect of IFN-α to increase ISG expression both *in vitro* and *in vivo*, suggesting that the combination of ME3738 and IFN might be useful therapeutically for patients with chronic hepatitis C.

Keywords: Human hepatocyte chimeric mouse; Interferon-stimulated genes.
Received 27 October 2009; received in revised form 26 September 2010; accepted 19 October 2010; available online 29 November 2010

* Corresponding author. Address: Department of Medicine and Molecular Science, Division of Frontier Medical Science, Programs for Biomedical Research, Graduate School of Biomedical Sciences, Hiroshima University, 1-2-3 Kasumi, Minami-ku, Hiroshima-shi 734-8551, Japan. Tel.: +81 82 257 5190; fax: +81 82 255 6220.
E-mail address: chayama@hiroshima-u.ac.jp (K. Chayama).

Abbreviations: HCV, hepatitis C virus; HSA, human serum albumin; IFN, interferon; IL, interleukin; ISG, interferon stimulated gene; MxA, myxovirus resistance protein A; OAS, oligoadenylate synthetase; PKR, double stranded RNA-dependent protein kinase; PCR, polymerase chain reaction; SCID, severe combined immunodeficiency; uPA, urokinase-type plasminogen activator; USP18, ubiquitin specific peptidase 18.

Introduction

The hepatitis C virus (HCV) infects an estimated 170 million people worldwide [1] leading to chronic hepatitis, liver cirrhosis, and hepatocellular carcinoma [2,3]. To date, the most effective therapy for viral clearance is a 48- or 72-week combination therapy of pegylated interferon (IFN)-α and ribavirin. However, successful eradication of the virus is achieved in only about 50% of treated patients [4–6]. Moreover, therapy induces significant adverse effects, such as fever, fatigue, and anemia [4], resulting in poor tolerability. More effective and less toxic treatment is, therefore, desired.

ME3738 (22β-methoxyolean-12-ene-3β, 24-diol), a derivative of soyasapogenol B [7], attenuates liver disease in several animal models of acute and chronic liver injury induced by concanavalin A, ethanol, lithocholate, and bile duct ligation [8–12]. ME3738 induces interleukin (IL)-6 expression, and serum amyloid A and α1-acid glycoprotein act as downstream targets of the IL-6 signal to protect against concanavalin A-induced liver injury [8–10]. The drug also prevents the progression of hepatic fibrosis in rats with bile duct ligation through suppression of activation and collagen synthesis of hepatic stellate cells [12].

Recently, Hiasa et al. reported that ME3738 inhibited HCV replication by enhancing IFN-β production using the HCV full-length binary expression system that uses full-length genotype 1a HCV complementary DNA plasmid with a T7 promoter sequence and an adenoviral vector expressing T7 polymerase [13]. However, it is not clear if the production of IFN-β and subsequent expression of IFN-stimulated genes (ISGs) was induced by the transcribed HCV genomes through detection by innate

ELSEVIER

Research Article

immune system receptors, including RIG-I. In addition, it is also not clear whether ME3738 has anti-viral effects on genotype 1b HCV, which is the most common and most IFN-resistant genotype in Japan [14].

Recently, HCV-infected mice have been developed by inoculating HCV-infected human serum into urokinase-type plasminogen activator (uPA)-severe combined immunodeficiency (SCID) mice engrafted with human hepatocytes [15,16]. We and other groups had reported that this mouse model is useful for evaluating anti-HCV drugs such as IFN-α and anti-NS3 protease *in vivo* [17–19].

In the present study, we investigated the effects of ME3738 on HCV replication both *in vitro* and *in vivo* using the genotype 1b HCV replicon and HCV-infected human hepatocyte chimeric mice. The results demonstrate that ME3738 itself had an inhibitory effect on HCV replication, and when combined with IFN, ME3738 enhanced the anti-HCV effect of IFN by up-regulation of ISGs, such as oligoadenylate synthetase (*OAS*) *1*, myxovirus resistance protein A (*MxA*), and *ISG15* in HCV replicon cells. We also showed that the combination therapy increased *OAS1*, RNA-dependent protein kinase (*PKR*) and ubiquitin specific peptidase 18 (*USP18*) expression levels, and reduced virus levels effectively without liver cell damage in human hepatocyte chimeric mice.

Material and methods

Cell culture

Cells supporting replication of the genotype 1b-derived subgenomic HCV replicon, ORN/3-5B/KE cells [20] (kindly provided by N. Kato, Okayama University, Japan) and Con-1 cells [21], were cultured in Dulbecco's modified Eagle's medium (Gibco-BRL, Invitrogen Life Technology, Carlsbad, CA) supplemented with 10% fetal bovine serum, non-essential amino acids, glutamine, penicillin, and streptomycin (complete DMEM) in the presence of G418 (300 μg/ml; Geneticin, Invitrogen, Carlsbad, CA). ORN/3-5B/KE and Con1 replicon cells (2×10^4) were seeded onto 12-well plates and incubated for 3 days with or without ME3738 (Meiji Seika Kaisha, Tokyo, Japan) [9], human IFN-α (Dainippon Sumitomo Pharma Co., Tokyo), or the combination of both drugs.

Quantitation of HCV RNA and ISG mRNAs

RNA extraction and quantitation of HCV by real-time polymerase chain reaction (PCR) were performed as described previously [19]. Briefly, RNA was extracted from mice serum, livers, or cellular lysate using SepaGene RVR (Sankojunyaku, Tokyo, Japan) and reverse transcribed with a random hexamer and a reverse transcriptase (ReverTraAce; TOYOBO, Osaka, Japan) according to the instructions provided by the manufacturer. Quantitation of HCV RNA was performed using the Real-Time PCR system (Applied Biosystems, Foster City, CA). The primers used for amplification were 5′-GAGTGTCGTGCAGCCTCCA-3′ and 5′-CACTCGCAAGCAC CCTATCA-3′. Quantitation of ISGs (*OAS1*, *MxA*, *PKR*, *USP18* and *ISG15*) was performed using real-time PCR Master Mix (TOYOBO) and TaqMan Gene Expression Assay primer and probe sets (PE Applied Biosystems, Foster City, CA). Thermal cycling conditions were as follows: a precycling period of 1 min at 95 °C followed by 40 cycles of denaturation at 95 °C for 15 s and annealing/extension at 60 °C for 1 min. Each ISG expression level was expressed relative to the endogenous RNA levels of the housekeeping reference gene glyceraldehyde-3-phosphate dehydrogenase (*GAPDH*).

Luciferase reporter assay

After 72 h of IFN and/or ME3738 treatment, ORN/3-5B/KE cells were harvested with Renilla lysis reagent (Promega, Madison, WI) and subjected to the luciferase assay according to the manufacturer's protocol.

Western blotting

The cells were ruptured with 250 μl lysis buffer [10 mM Tris/HCl pH 7.4, 140 mM NaCl and 0.5% (v/v) NP-40] followed by centrifugation for 2 min at 15,000g. Cell lysates were subjected to Western blotting using antibodies against NS3 (Novocastra Laboratories, UK) and β-actin (Sigma, Tokyo, Japana) as described previously [22].

WST assay

Cell viability was determined by employing tetrazolium salt, WST-8, using the WST-8 Cell Proliferation Assay Kit (Dojindo Laboratories., Kumamoto, Japan), according to the instructions provided by the manufacturer.

Human serum samples

Human serum samples containing high titers of genotype 1b HCV (2.2×10^6 copies/ml) were obtained from a patient with chronic hepatitis after obtaining written informed consent. Aliquots were stored in liquid nitrogen until use.

Animal treatment

All animal protocols in this study were in accordance with the guidelines of the local committee for animal experiments and under approval of the Ethics Review Committee for Animal Experimentation of the Graduate School of Biomedical Sciences, Hiroshima University. We transplanted human hepatocytes into $uPA^{+/+}/SCID^{+/+}$ mice as described previously [16]. All mice used in this study were transplanted with frozen human hepatocytes obtained from the same donor. Mice were injected intravenously with 50 μl of HCV-positive human serum samples. Six weeks after HCV infection, mice were fed a normal chow containing 0.15% (w/w) ME3738 for 4 weeks, with or without IFN-α. IFN-α-treatment was provided daily by intramuscular injection of diluted IFN solution. Serum samples were collected every week, and human serum albumin (HSA) concentration and HCV RNA were measured. Mouse serum concentrations of HSA, which correlate with the repopulation rates, were measured as described previously [16]. Serum ME3738 concentrations were measured by liquid chromatography/mass spectrometry/mass spectrometry. After the fourth week of treatment, mice were sacrificed, and livers were either fixed with 4% buffered-paraformaldehyde for histological examination or frozen immediately in liquid nitrogen to measure HCV core antigen. To investigate the expression of ISGs in mouse livers, mice were kept for 1 week with or without 0.45% (w/w) ME3738 and then given a single injection of 1500 IU/g IFN-α. Four hours after injection, mice were sacrificed and liver samples were collected.

Quantitation of HCV core antigen in the mouse liver

Livers were homogenized in phosphate-buffered saline with 1% Triton X-100, 0.1% SDS, and 0.5% sodium deoxycholate. The homogenates were centrifuged at 20,000g for 30 min. HCV core antigen levels in the supernatant of liver homogenates were measured using enzyme immunoassay as described previously [23].

Statistical analysis

All data are expressed as mean ± SD. Levels of HCV RNA and ISG mRNAs were compared using the Mann–Whitney *U*-test. A p value less than 0.05 was considered statistically significant. All statistical analyses were performed with SPSS 14.0 software (SPSS, Tokyo, Japan).

Results

Antiviral activity of ME3738 on HCV subgenomic replicon

The effect of ME3738 on HCV replication was analyzed *in vitro* using subgenomic HCV replicon cells possessing the luciferase reporter. ORN/3-5B/KE cells were treated with either IFN-α or ME3738 for 72 h. The luciferase reporter assay demonstrated that the HCV RNA replication level decreased depending on the